REPUBLIQUE ALGERIENNE DEMOCRATIQUE ET POPULAIRE
MINISTERE DE L'ENSEIGNEMENT SUPERIEURE ET DE LA RECHERCHE SCIENTIFIQUE

UNIVERSITE ABOU-BEKR BELKAID – TLEMCEN

MEMOIRE

Présenté à :

FACULTE DES SCIENCES – DEPARTEMENT DE PHYSIQUE

Pour l'obtention du diplôme de :

MASTER EN PHYSIQUE

Spécialité : Physique médicale

Par :

Ms Kawther benrezkallah

Sur le thème

Modeling behavior of radiation beams in radiotherapy using AI

Soutenu publiquement le 03 juillet 2025 à Tlemcen devant le jury composé de :

Mr KARA-ZAITRI Kamel	MCA	Université de Tlemcen	Président
Mr BOUFATEH Mohammed Reda	MCA	Université de Tlemcen	Encadrant
Mr BENDAHMANE Mohammed Fawzi	MCA	Université de Tlemcen	Examinateur
Dr. BOUCHIKHI Asma	Docteure	CAC Tlemcen	Examinatrice
Ms BENSABER Fatima Zahra	Doctorante	Université de Tlemcen	Co-encadrante

Année Universitaire : 2024 ~ 2025

n

Dedication

I dedicate this Thesis to:

My loving parents, Ahmed and Benrezkallah Fatiha, whose sacrifice, love, and constant support have been the foundation of my journey. I will always be grateful for their constant encouragement and sincere prayers.

To my dear siblings, Hadjer, Abdelhadi, Iman, Younes, and Deyfallah, for their constant encouragement and support.

To my sister-in-law, Sarah, and my brothers-in-laws, Mohammed and Said, for their encouragement and kindness.

To my dear nieces and nephews, Amina, Yasser, Nabia, Ismail, Iline and Shamse Abrar, whose smiles inspire me and bring me boundless joy.

To my entire family, for being a source of strength, love, and support.

To my university colleagues and all my professors, whose guidance and friendship have made my student life worthwhile.

Acknowledgments

I would like to express my heartfelt gratitude to:

First and foremost, my supervisor, Boufatah Mohammed Reda, and my co-supervisor, Bensabar Fatima Zahra, for their invaluable guidance, insightful advice, and unwavering support throughout the preparation of this thesis. Their expertise, patience, and encouragement have been instrumental in shaping this work.

I also extend my sincere thanks to the jury members, president Kara-Zaitri Kamal, examiners Bendahmane Mohammed Fawzi and Bouchikhi Asma , for taking the time to review and evaluate my work.

I would also like to sincerely thank all the professors who generously shared their knowledge, and my colleagues at university for their collaboration, support, and enriching discussions.

Finally, I am deeply grateful to my family and friends for their endless encouragement, patience, and love throughout this journey.

Abstract:

Radiation therapy (RT) playing an important role in cancer treatment modality that using high-energy radiation to killing tumors without damaging healthy tissues (OARs). However, still achieving optimal beams radiation delivery accuracy remains a significant challenge. The advanced techniques such as VMAT, IMRT, IGRT have enhanced treatment precision , but still need improving incorporating new technologies .

Artificial intelligence, particularly ML and DL offers potential to improving revolution in RT. One of possible way is modeling behaviors of radiation beams. AI techniques enable to analysis of massive datasets and identify complex patterns that are difficult to detect by traditional methods.This thesis explores the application of AI in a part of modeling behaviors of radiation beams which is classifying OARs into categories.

The research focusing on using clinical data from real cases “ cavum cancer “ about 10 patients with one to three plans to develop an AI model for classifying OARs into : safe , medium risk , high risk , unknown (this for clinical volume which it varies from one plan to another) . The developed model using dose metrics such as maximum, mean, and median doses, along with anatomical structure types and other clinical variables to assess OAR risk levels. A CatBoost Classifier was employed and demonstrated excellent performance in terms of accuracy, recall, precision, and F1 score, ensuring reliable identification of high-risk cases—an essential requirement in medical decision-making.

Data preprocessing steps included handling class imbalance using Random Over Sampling, followed by feature selection and model training using the PyCaret library. The results indicate that the AI model successfully identifies all high-risk and medium-risk cases, with minimal false positives in the "Safe" category. Feature importance analysis revealed that dose-related parameters were the most influential in determining risk classification.

This study demonstrates how AI can support radiation oncologists and medical physicists in making more informed and efficient treatment decisions. By integrating AI into RT planning, this approach enhances the quality and safety of treatment plans, reduces planning time, and improves patient outcomes. Despite limitations related to dataset size and technical expertise, the findings underscore the promising role of AI in transforming radiotherapy workflows and advancing personalized cancer treatment.

KEYWORDS: Artificial Intelligence, Machine Learning, Deep Learning, Radiotherapy, Beam Modeling, Organ at Risk (OAR), Dose Prediction, Treatment Planning, CatBoost Classifier, Medical Physics.

The best way to predict the future is to create it."
— Peter Drucker

I. LIST OF ABBREVIATION:

ABBREVIATION	FULL FORM
AI	Artificial Intelligence
AAPM	American Association of Physicists in Medicine
AUC	Area Under the Curve
CBCT	Cone-Beam Computed Tomography
CNN	Convolutional Neural Network
CORSAIR	Dose–Volume Constraints for Organs at Risk
CT	Computed Tomography
DVH	Dose Volume Histogram
DIR	Deformable Image Registration
DL	Deep Learning
DMAX	Maximum Dose
DMEAN	Mean Dose
DMIN	Minimum Dose
EBRT	External Beam Radiotherapy
GAN	Generative Adversarial Network
GPU	Graphics Processing Unit
GY	Gray (Unit of Radiation Dose)
HI	Homogeneity Index
IMPT	Intensity-Modulated Proton Therapy
IMRT	Intensity-Modulated Radiotherapy
IGRT	Image-Guided Radiotherapy
KNN	K-Nearest Neighbors
MCC	Matthews Correlation Coefficient
ML	Machine Learning
MRI	Magnetic Resonance Imaging
OAR	Organ at Risk
PCA	Principal Component Analysis
PET	Positron Emission Tomography
PTV	Planning Target Volume
QA	Quality Assurance
RNN	Recurrent Neural Network
ROC	Receiver Operating Characteristic
RT	Radiotherapy
RBM	Restricted Boltzmann Machine
RELU	Rectified Linear Unit
SVM	Support Vector Machine
SBRT	Stereotactic Body Radiotherapy
SRS	Stereotactic Radiosurgery
TPS	Treatment Planning System
VMAT	Volumetric Modulated Arc Therapy

II. LIST OF FUGURES

- CHAPTER ONE :

- CHAPTER THREE:

- CHAPTER FOUR :

III. LIST OF TABLES

- CHAPTER ONE :

- CHAPTER THREE :

- CHAPTER FOUR :

INDEX

Index

GENERAL INTRODUCTION

General Introduction

Radiotherapy (RT) is an essential treatment for cancer that uses high-energy radiation to destroy cancer cells while sparing surrounding healthy tissue. Nevertheless, achieving optimal accuracy in radiation beam delivery remains a significant challenge. Novel methods such as Intensity-Modulated Radiotherapy (IMRT), Volumetric Modulated Arc Therapy (VMAT), and Image-Guided Radiotherapy (IGRT) have enhanced treatment accuracy, but further improvements are still required.

One of the most promising techniques for enhancing radiation therapy is the application of Artificial Intelligence (AI). AI techniques, particularly machine learning and deep learning. offer powerful tools for assessing large datasets and identifying complex patterns that can be utilized for the optimization of beam modeling in RT. Through the integration of AI, more personalized and accurate treatment plans can be developed, with overall better patient outcomes.

This thesis explores the application of AI for improving the modeling of radiation beams in RT. Specifically, objective is to explore how AI can be leveraged to optimize beam behaviors, which will lead to more precise treatment delivery.

Chapter 1 provides a review of the historical development of radiotherapy and the fundamental principles of radiation treatment. It begins with the initiation of radiotherapy, including the discovery of X-rays and radioactivity, and traces the evolution of RT methods such as IMRT, VMAT, and IGRT. The chapter further delves into recent developments in RT, covering proton therapy and other newer approaches.

In addition to the historical perspective, this chapter introduces the behavior of radiation beams, the factors that influence their behavior, such as radiation type and energy. It also discusses the key role of beam modeling in treatment plan optimization so that the tumor is properly dosed while side effects are kept to a minimum.

Chapter 2 provides a summary of the recent literature on AI applications in radiotherapy. The chapter begins with research methodology used to collect and analyze relevant studies on AI applications in RT, with an explanation of key terms like "AI in RT,"

"deep learning," "machine learning," and "beam modeling with AI." This chapter then presents findings from previous studies in the field, determining the merits and limitations of current solutions.

The third chapter focuses on the practical aspects of the research, namely the process of data collection, preprocessing, and initial classification of organs at risk (OARs) into appropriate risk categories. Data were collected from real clinical cases involving cavum cancer and extracted from the Eclipse/ARIA treatment planning system. The dataset includes dose-volume histograms, dose constraints, and anatomical details for each patient, and was organized into a structured format for AI training. The chapter also details the calculation of the Homogeneity Index (HI), an important indicator of treatment plan quality, and presents the classification of OARs into serial and parallel types.

Chapter four is the final chapter and it’s dedicated to the development and implementation of the AI model for beam behavior prediction and treatment evaluation. It describes the selection of appropriate algorithms, model architecture, and training strategies. Evaluation metrics such as dose compliance and HI performance are used to assess the model's effectiveness. The chapter concludes by discussing the model's clinical relevance, its limitations, and prospects for future improvements. The overarching goal is to propose a tool that supports radiation oncologists and medical physicists in making more informed and efficient treatment decisions.

The final section presents the code implementation of the proposed AI model. This part translates the theoretical and methodological concepts into a practical application. The code is designed to analyze radiotherapy data and assist in predicting dose distribution for OARs and classifying the organs into four categories: safe, medium risk, high risk, and unknown, based on the mean dose. It serves as the technical foundation supporting the model’s objectives and functionalities.

CHAPTER ONE

HISTORY AND BASIC CONCEPTS OF RADIOTHERAPY

1. HISTORY AND BASIC CONCEPTS OF RADIOTHERAPY:

1.1 Introduction:

In this chapter we present an overview of the history of radiation therapy from the discovery of X-rays until the present day. we will examine how radiation beams work and explore innovations such as VMAT, IMRT, and IGRT in radiotherapy treatment. Finally, there is some discussion on the growing use of AI for ensuring greater precision and speed in radiation therapy.

1.2 Radiotherapy: Definition and historical context:

1.2.1 History:

In 1895 a scientist named Wilhelm Conrad Röntgen discovered X-rays, when he was studying new type of radiation able to go through screens of notable thickness and the "X-rays "name came from the fact that their nature was unknown. (1).

Since January 1896 physicians and physicists use X-rays on patients. This was the birth of radiology, but they observed skin erythema, which led to the idea of using X-rays against a variety of lesions. However, in June 1896 the first patient was treated by radiotherapy after that, J.J.Thomson showed that these rays were able to ionize Gaz and then in 1897 led to the discovery of electrons. this pivotal moment in science opened the door to further research into atomic structure and radioactivity. Rontgen's discovery caused a major upheaval in physics and medicine. (2) (3) .

This important discovery enabled the visualization of internal structures without invasive procedures transformed diagnostic practices and laid the ground work . for modern imaging techniques , his initial experiments included taking the first X-ray photographs, such as the famous image of his wife's hand in Fig.1 , which showcased the potential of this new technology in revealing anatomical details previously hidden from view .

As research progressed, radiation therapy underwent radical changes. Early treatments relied on simple and primitive methods, but these began to improve thanks to continuous technological innovation. These innovations included: Three-Dimensional Conformal Radiotherapy (3D-CRT), Intensity-Modulated Radiotherapy (IMRT), Image-Guided Radiotherapy (IGRT), Proton Therapy, Dynamic Tracking Radiotherapy, Stereotactic Radiosurgery (SRS), and Stereotactic Body Radiotherapy (SBRT). Then the latest developments contributed such as Adaptive Radiotherapy (ART), Biologically Modulated Radiotherapy, AI-Based Radiotherapy, and Fast Neutron Therapy In expanding the scope of accuracy, effectiveness, and customization of treatment options. (4)

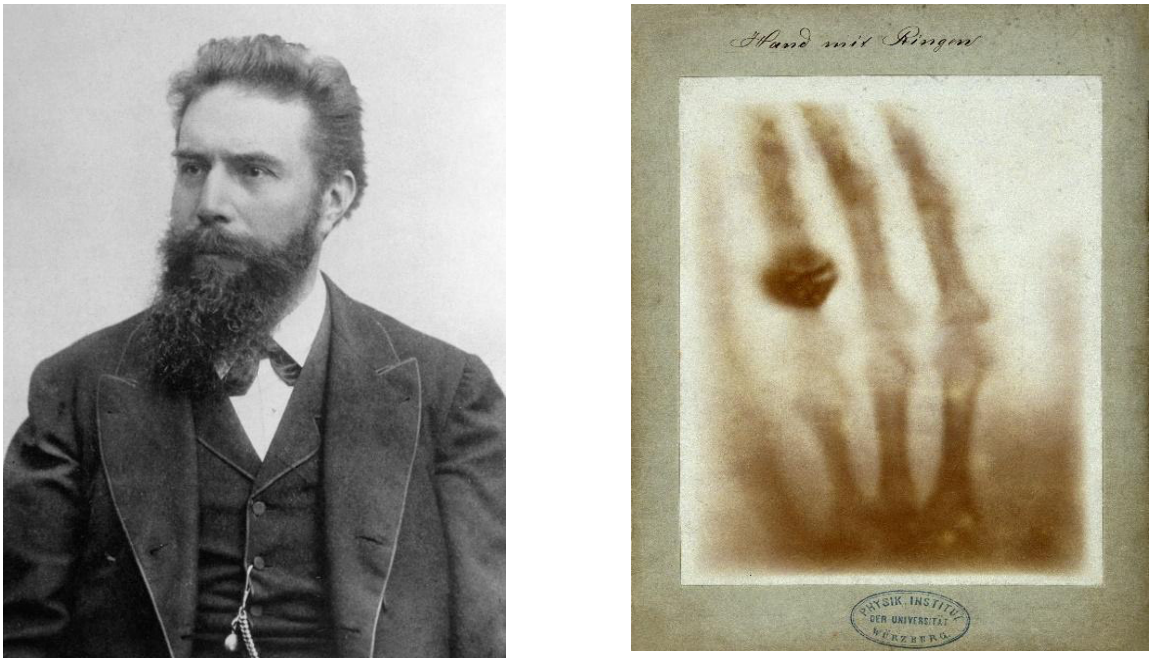

figure 1: Wilhelm Conrad Roentgen received the Nobel Prize in 1901 for his discovery of X□rays. He took the first X□ray of his wife's hand (Anna Bertha Ludwig), which showed her wedding ring and the bones of her fingers and some soft tissues. Source: Image adapted from https://en.wikipedia.org/wiki/Wilhelm_Röntgen

1.2.2 Evolution of radiotherapy techniques :

1.2.2.1 Three-dimensional conformal radiation therapy (3D-CRT) :

Three dimentional conformal radiation therapy or known as 3D-CRT , the first radiation thrapy where the size and shape of the tumor , as well as normal organs are defined in 3D using imaging technologies like CT scans , MRI , PET scans , PET-CT scan and ultrasound .

The beams are positioned to deliver a specific radiation dose to the tumor while protecting organs at risk. and is commonly used in the treatment of brain, head and neck, liver, lung, and prostate cancers (4, 7).

1.2.2.2 Intensity modulated radiation therapy (IMRT):

In 1990s IMRT was developed and is one of the most advanced forms of 3D conformal RT, it uses multiple small radiation beams, also allows for the precise delivery of radiation dose to tumors while minimizing exposure to surrounding healthy tissues, it's particularly beneficial for complex tumor shapes and locations close to sensitive structures (5, 6).

1.2.2.3 Image-guided radiation therapy (IGRT):

IGRT is a highly advanced radiation therapy modality, combines frequent imaging to enhance radiation delivery accuracy and precision. It's critical to precisely position the patient and direct the radiation beams toward the tumor, while avoiding any exposure to adjacent healthy tissues [4].

1.2.2.4 Volumetric Modulated Arc Therapy VMAT:

Volumetric Modulated arc therapy, a type of advanced treatment technique, delivers treatment using a linear accelerator with a cone beam that continuously rotates around the patient. Each rotation is called an arc, and one or more arcs can be used. Each rotation also includes the synchronized movement of the gantry , MLC, and dose rate. This technique provides highly conformal dose distribution, which improves target coverage and preserves healthy tissue. VMAT is one of the best treatment techniques because it takes less time and offers better efficacy. [11 ,12].

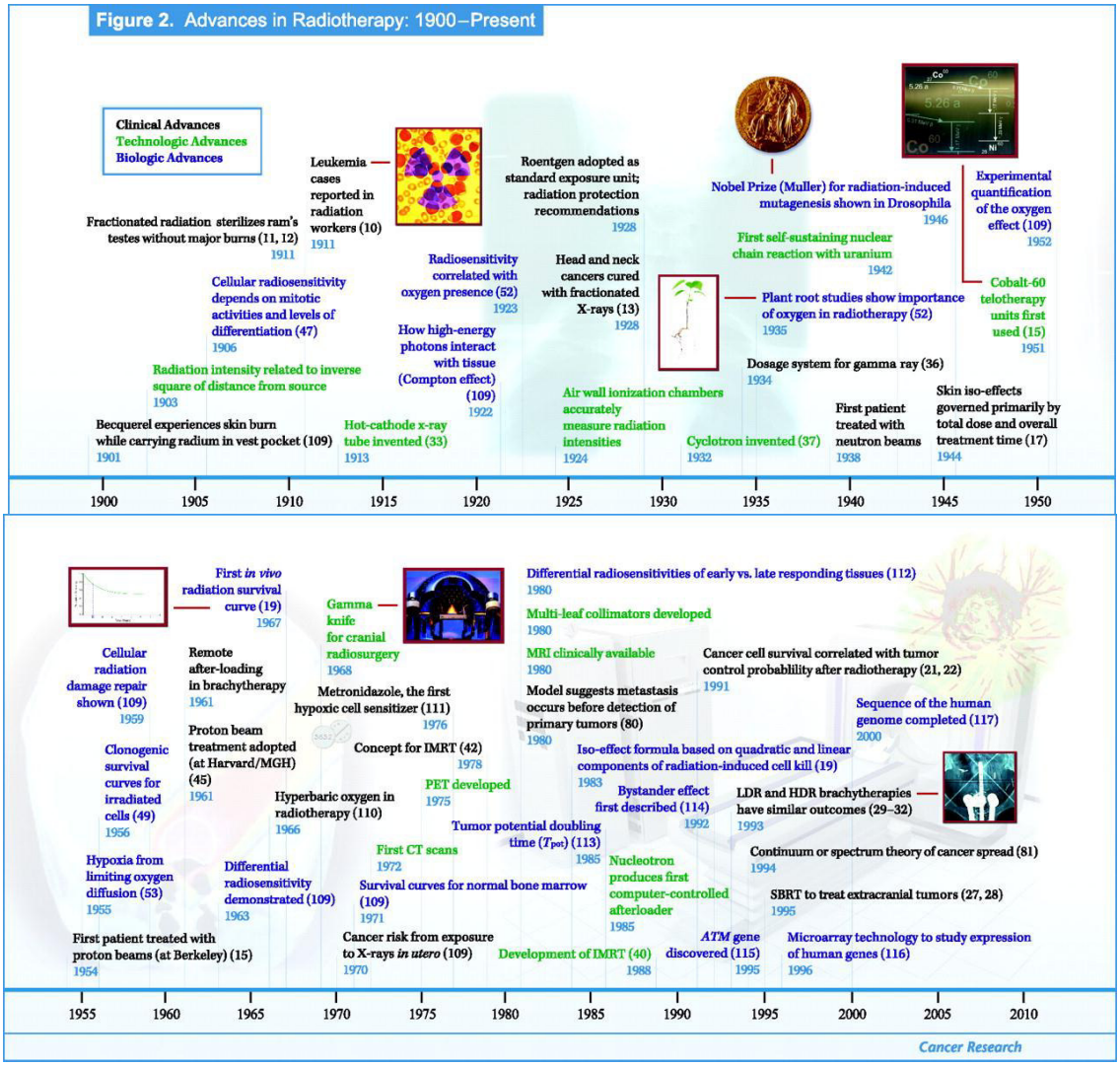

Figure 02: A time-line of clinical, technologic, and biological advances in radiation oncology.

1.2.3 Recent advancement with proton therapy and other advanced techniques:

1.2.3.1 Definition of proton therapy :

Proton therapy also known as proton beams therapy defined as advanced type of radiation treatment that uses protons rather than X-rays to treat cancer . this therapy have the ability to delive high dose of radiation to tumors with minimal damage to surrounding healthy tissues. [15]

Wilson was the first one who recognize the potential of physical characteristics of proton for cancer treatment in 1946 [16] . years by years of developing scientist find many advanced techniques such as :

1. ***Passive scattering proton therapy (PSPT) :***

   This technique uses scatterers to spread out the proton beam to cover the entire tumor volume. PSPT is commonly used for treating large and irregularly shaped tumors.

2. ***Pencil Beam Scanning (PBS) :***

   Andrew Lee, M.D., MPH, medical director of Texas Center for Proton Therapy served as the first physician in North America to treat patients with pencil-beam scanning in Texas center website mentioned that :

   pencil-beam scanning, also known as spot-scanning, is an advanced form of proton therapy this technique uses a narrow proton beam that is magnetically steered across the tumor in a raster pattern. that delivers ultra-fine, targeted doses of radiation to each layer of a patient's tumor that making it ideal for for treating tumors located near critical structures .

3. ***Intensity-Modulated Proton Therapy (IMPT):***

   According to the abstract by H. M. Kooy and C. Grassberger, Intensity-"Modulated Proton Therapy (IMPT) is an advanced form of proton therapy that uses electromagnetic spatial control of well-defined "pencil beams" of protons, varying their energy and intensity to precisely modulate the dose delivered to different parts of the tumor. IMPT improves upon traditional X-ray intensity-modulated radiotherapy by allowing dose modulation both along the beam axis and laterally within the field, resulting in better sparing of normal tissues and the potential for higher tumor doses." [17].

4. ***Adaptive Proton Therapy (APT):***

"Adaptive radiation therapy is technique that applied to consider changes in patient anatomy during the course of fractionated treatment delivery. Adaptation is particularly important in proton therapy where small changes in patient anatomy can lead to significant dose perturbations due to the dose conformality and finite range of proton beams. "(Paganetti et al., 2021) . [18]

1.2.4 Recent Advancements in Proton Therapy:

Recent advances in proton therapy include :

- Enhanced imaging capability improves tumor imaging and allows precise dose delivery with adaptation to anatomical change during treatment .
- Nanoparticle radiosensitization enhances the biological effectiveness of proton therapy by inducing radiation damage in tumor cells selectively .
- Expanded clinical use includes more cancer sites and patient groups, with an aim to reduce side effects and improve outcome. [8, 9, 10, 19 , 20, 21 , 22].

1.3 An Overview of Behavior of Radiation Beams :

1.3.1 Definition of Radiation Beams:

Radiation beams refer to energy or particle streams directed along a defined path. They can be electromagnetic beams—light, X-rays-or the beams of particles e.g., electrons and protons (1, 2, 7). Grasping how these behave is very important in varied fields such as medical imaging, radiation therapy, and nuclear physics. Radiation beams are the mainstays of external beam radiotherapy, for cancer treatment within radiotherapy, invalidating or killing cancer cells by interaction with biological tissue (3, 4). The positioning of a source of radiation at a distance from the phantom or patient so that the target inside the patient is irradiated with an external radiation beam (4, 5). These may be photon beam, electron beam, proton beam, and heavy ion beam, all varying with physical and biological properties (6, 7).

1.3.2 Factors Influencing Radiation Behavior:

1.3.2.1 Types of Radiation Beams:

1.3.2.1.1 Electromagnetic Radiation:

- Gamma_Rays: by nuclear transitions they produce a high energy photons .which have high penetration power however are attenuated by dense materials like lead or concrete. Their wavelength is approximately 10 picometers. [6]
- X-rays: Similar to gamma rays but typically produced by electronic transitions. They also penetrate materials well, and are used extensively in medical imaging. [8]

- Visible light: moving at different speeds depending on the medium, sometimes slows down in denser materials such as glass or water, then we having phenomena such as refraction. [7]

Particle Radiation:

- Alpha radiation: consists of helium nuclei (two protons and two neutrons). Its penetration power is low and it shall be shielded by a paper or skin. [6]
- Beta Radiation: Consists of electrons emitted from atomic nuclei. It has moderate penetration and can be stopped by a few millimeters of wood or metal. [6]

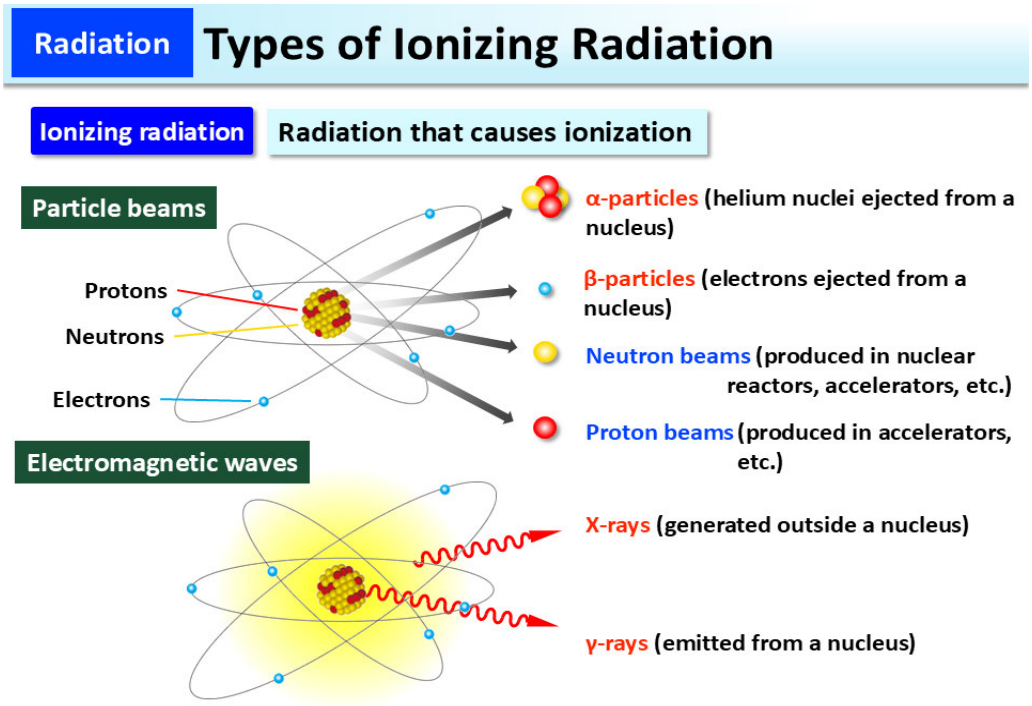

Figure 3 : Types of Ionizing Radiation, Ministry of the Environment, Japan. BOOKLET to Provide Basic Information Regarding Health Effects of Radiation, 5th edition, Chapter 1. Retrieved from https://www.env.go.jp/en/chemi/rhm/basic-info/1st/01-03-03.html

This diagram explain the major types of ionizing radiation, such as particle beams (α-particles, β-particles, neutron beams, proton beams) and electromagnetic waves (X-rays and γ-rays), with their respective origins and characteristics.

1.3.2.2 Energy Level:

High-energy radiation (e.g., gamma rays) penetrates materials more effectively than low-energy radiation (e.g., alpha particles).

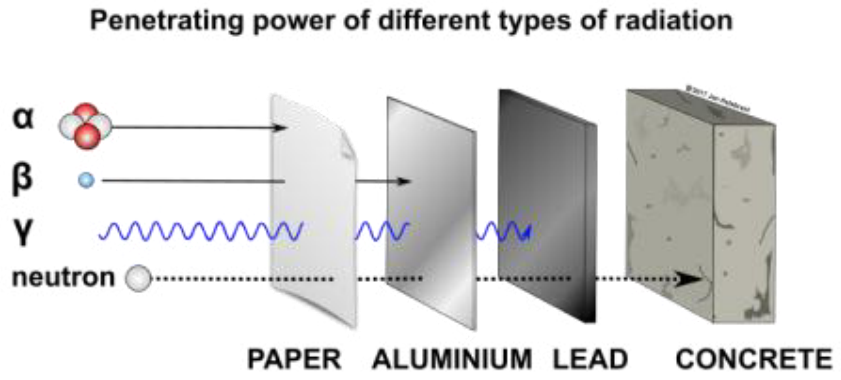

Figure 04 penetrating power of different types of radiation.

1.3.2.3 Medium Properties:

The density and atomic composition of the material be irradiated having an important role of the way that how it absorbs or scatters radiation. [9]

1.3.2.4 Beam Quality:

The quality of the primary beam (energy spectrum) governs the degree of scatter produced in the course of its interaction with any material. [5] .

1.3.3 Importance of Beam Modeling in Treatment Planning:

In radiation therapy beam modeling is important in Treatment Planning, it's directly influences the accuracy and effectiveness of dose delivery to tumors while minimizing exposure to surrounding healthy tissues. Here are key aspects highlighting its importance:

1.3.3.1 Accuracy in Dose Calculation:

1.3.3.1.1 Monte Carlo Simulations:

Beam modeling makes way for sophisticated Monte Carlo (MC) simulations, known for their high accuracy in calculating radiation doses delivered to the patients. These simulations include the complex radiation-matter interactions, which result in very precise dose distribution, an essential factor for effective treatment planning. [1]

1.3.3.1.2 TPS Commissioning:

Accurate beam models are extremely important for the commissioning of the TPS; only then can the systems predict reliably the dose from different radiation beams. The whole process involves extensive validations and tests of beam models versus clinical data. [1 2]

1.3.3.2 Customization for Specific Treatment Techniques:

1.3.3.2.1 Adaptation to Varied Treatment Modalities:

Different treatment techniques like IMRT and VMAT use beam models that will best validate their individual characteristics. The custom models thus help optimize the treatment plans according to the patient's anatomy and tumor location. [2 4]

1.3.3.2.2 *Improved Treatment:*

Clinically optimized beam models achieve treatment plans that conform better to realistic dosimetric measurements, thereby improving the treatment quality a patient finally receives. [2]

1.3.3.3 Efficiency in Treatment Planning Workflow:

1.3.3.3.1 Reducing Commissioning Period:

Template beam models may greatly facilitate the commissioning process since it provides a good initial working point for further optimization. Consequently, a great reduction in time for the development and validation of new beam models would allow clinics to begin using new technologies much faster. [2 4]

1.3.3.3.2 Facilitation of Multi-Institutional Collaboration:

Standardized beam models can offer consistency between institutions in data sharing and treatment planning collaborative protocols, thus giving special consideration to multi-vendor opportunities where varied equipment is used. [2]

1.3.3.4 Paciente Safety Enhancement

1.3.3.4.1 Error Minimization:

Accurate beam modeling is employed to minimize any possible errors in dose delivery, which helps to ensure patient safety. This approach ensures that the planned doses match the actual delivered doses, significantly reducing the risk of under- or over-treatment [3 4].

1.3.3.4.2 Model Validation Against Clinical Data:

Continuous validation on clinical outcomes ensures that beam models can identify discrepancies and correct them that ensure patient safety enhancement and treatment efficacy. [1 2].

1.4 Artificial intelligence in radiation therapy:

1.4.1 basic concepts of machine learning and deep learning:

1.4.1.1 Introduction:

Machine learning and deep learning are related. They are sub-domains of artificial intelligence, but they depend on different prediction methods. These techniques require large datasets to develop accurate learning models.

Although these two terms refer to two distinct methods, they are often confused.

Machine learning is a set of modifiable algorithms or source codes that make the machine more independent and autonomous. Implementing this technology requires the existence of organizational data.

Machine learning is carried out via controllable data.

Deep learning is a sub-set of machine learning based on deep neural networks. Thanks to deep learning, the system itself can identify distinctive features in data without prior classification.

Table 1: Comparison between machine learning and deep learning

	MACHINE LEARNING	**DEEP LEARNING**
THE DATAS	• structured (organized) • controllable	• unstructured (unorganized) • uncontrollable
ALGORITHMS	• Modifiable	• deep neural networks
USEFUL FOR	• simple data	• complex data

1.4.1.2 Machine learning algorithms:

Machine learning is a very broad field that encompasses many algorithms. There are two basic methods: supervised learning and unsupervised learning, as well as semi-supervised learning (through reinforcement), which is considered complementary to supervised learning.

Before diving into the details, I will explain a term that I will use often: Dataset.

A Dataset is a set of values associated with each other and contains two types of variables:

- Dependent variable X: also called features.
- Independent variable Y: also called target.

1.4.1.2.1 Supervised learning:

This is the supervision of machine learning by showing examples of data to be processed.

In general, the machine can learn a relationship between input and output by analyzing the examples provided.

There are four essential elements for supervised learning:

- Provide the machine with examples to train it.
- Choose a model and train it with random data.
- The Cost Function.
- Find the model parameters that reduce the Cost function by developing an algorithm.

Supervised learning solves two types of problems:

"Classification" and "regression."

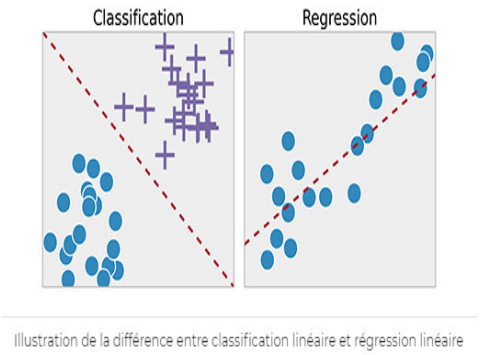

Figure 3: The difference between linear classification and linear regression

1.4.1.2.1.1 Classification:

This technique is applied to discrete variables.

The main purpose of classification control is to define rules that enable objects to be classified.

There are many classification methods, each of which specializes in a specific type. Therefore, it is important to choose the appropriate method before starting the classification process. These methods are as follows:

1.4.1.2.1.1.1 Decision tree:

A decision tree is a series of rules for solving classification problems, adapted to qualitative data. It takes the form of a tree and also consists of:

- Nodes: for testing variables.
- Branches: each variable has its own branch.
- Leaves: each leaf identifies a specific category.

A). How to build a decision tree?

To build a decision tree, you need to go through three steps, which are as follows:

a. Define the problem:

This involves asking a question to make the appropriate decision. For example:

Am I going to the beach?

b. Identify the branches:

By specifying the parameters, conditions, and data you have available in order to build a basis for decision-making.

Continuing with the same example above, the parameters here are weather parameters.

c. Make your decision: The decision here will be “yes” or “no.”

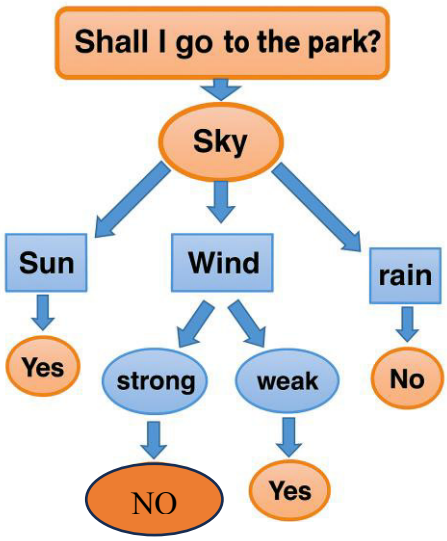

Figure 4: Example of a decision tree

There are a large number of these standards, the most commonly used being: CART and C5.0, etc.

1.4.1.2.1.1.1.1 Classification and Regression Tree (CART):
This algorithm is valid for both classification and regression. It is an algorithm that allows the response to be expressed as “yes” or “no.”

Each root node represents a single input variable (x) and a split point on that variable (assuming the variable is numerical).

The leaf nodes of the tree contain an output variable (y) that is used to make a prediction.

Given a dataset with two inputs (x) of height in centimeters and weight in kilograms, the output is gender as male or female. [1]

The GINI index is commonly used in this algorithm because it indicates the purity of the nodes, so that the smaller the GINI index, the purer the nodes.

The GINI index is considered a separation criterion. It is defined by the following equation:

$$\boldsymbol{G = 1 + \sum_{k=1}^{c} P^2(k/P)} \qquad (1.1)$$

where: P(k/P): is the probability of selecting an element from class c in P (P is the subset of the node's repetition).

In addition to being an indicator of purity, it is also useful for determining the correct size of the tree, as well as being important in choosing which variable to segment among the variables.

1.4.1.2.1.1.1.2 SHANNON's Entropy Algorithm:

Entropy is considered an algorithm for measuring uncertainty.

It therefore allows us to measure the average amount of information in a set of events and to measure its uncertainty. It is denoted by H [2]:

$$\boldsymbol{H = \sum_{i\in l}^{\infty} \left(P_i . Log\left(\frac{1}{P_i}\right)\right) = \sum_{i\in l}^{\infty} (P_i . Log(P_i))} \qquad (1.2)$$

Shannon's algorithm associates the concept of information with the measurement of uncertainty.

1.4.1.2.1.1.1.3 K nearest neighbors KNN:
KNN is one of the simplest algorithms in supervised learning. It is used to classify data and is also valid for regression problems.

This algorithm identifies, stores, and classifies all available possibilities by checking its nearest neighbor K to determine which class the object to be classified belongs to.

To find the classification of the yellow circle (in Figure 5), you must first select the number of neighbors K, then calculate the distance between them, and then sort and organize the calculated distances in ascending order.

Among these K neighbors, compare these distances and find the points that have the closest distance, and select the category to which it belongs.

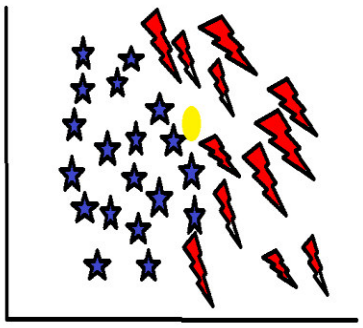

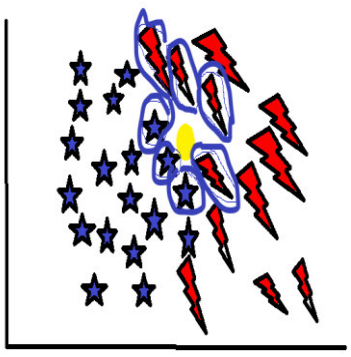

Figure 5: Example of the KNN method

1.4.1.2.1.1.2 Naive Bayesian:

This is a simple classification model that belongs to the family of linear classifiers. It is often used to classify text and spam. Naive Bayesian is suitable for parameter problems. It is based on Bayes' theorem based on conditional probability.

The theorem formula is as follows:

$$\boldsymbol{P\,(A/B) = \frac{P(B/A)P(A)}{P(B)}} \qquad \boldsymbol{(1.3)}$$

A, B: events.

P(A), P(B): the probability of event A, B.

P(A/B): the probability that event A will occur given that event B has already occurred.

1.4.1.2.1.1.3 Support vector machine (SVM):

The basic principle of SVM is to simplify the identification problem into a linear problem of finding the best hyperplane. Two ideas or tips for achieving this goal:

The first key idea is the notion of maximum margin. The margin is the distance between the separating boundary and the closest samples. These are called support vectors. In SVMs, the separating boundary is chosen as the one that maximizes the margin. This choice is justified by Vapnik-Chervonenkis theory (or statistical learning theory), which shows that the maximum margin separating boundary has the smallest capacity. The problem is to find this optimal separating boundary from a training set. This is done by formulating the problem as a quadratic optimization problem, for which there are known algorithms.

In order to be able to handle cases where the data are not linearly separable, the second key idea of SVMs is to transform the representation space of the input data into a higher-dimensional space (possibly of infinite dimension), in which it is likely that a linear separator exists. This is achieved using a kernel function, which must meet certain conditions and has the advantage of not requiring explicit knowledge of the transformation to be applied for the change of space. Kernel functions allow a scalar product in a high-dimensional space, which is costly, to be transformed into a simple point evaluation of a function. This technique is known as the kernel trick. [3]

1.4.1.2.1.2 Regression:

Regression is a supervised learning technique used to determine the relationship between variables in order to make predictions. It applies to continuous variables with an infinite number of values.

In regression, we plot a graph between the variables that best fit the given data points. Using this graph, the machine learning model can make predictions about the data. In simple terms, “Regression shows a line or curve that passes through all the data points on the target predictor graph in such a way that the vertical distance between the data points and the regression line is minimal.” The distance between the data points and the line indicates whether a model has captured a strong relationship or not. [4]

1.4.1.2.1.2.1 Linear regression:

This is an easy method to apply, showing the linear relationship between the target variables Y and the predictor variables X. When there is only one X input, it is called simple linear regression; otherwise, it is called multiple linear regression.

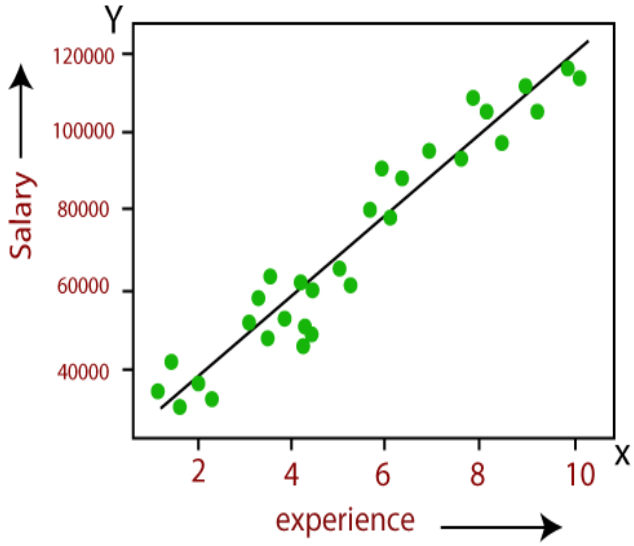

Figure 6: Linear regression

Linear regression is expressed in the following form:

$$\boldsymbol{Y = aX + b + e} \quad (1.4)$$

Y: the target variable (dependent)

X: the predictive variable (independent)

a: linear coefficient (slope)

b: linear coefficient (intercept)

e: the error term

To study the model, the errors must be independent variables.This can be written in vector form as follows:

$$\boldsymbol{\widehat{Y} = h_\theta (X) = \theta . X} \quad \textbf{(1.5)}$$

Where:

h: the hypothesis function.

1.4.1.2.1.2.2 Logistic regression:

This is a statistical method used to predict outcomes based on observations in a data set.

Logistic regression estimates the probability of events occurring and determines the relationship between characteristics and the probability of the event occurring.

In order to obtain high accuracy in estimating probabilities, a large data set must be provided.

For example, logistic regression can answer the following types of questions: What is the probability that a student will pass or fail a bachelor's degree exam? Or what are the chances of winning in sports betting?

There are two types of logistic regression:

• Binary logistic regression: the results are in binary form, such as “Yes or No,” “True or False,” or “0 or 1.”

• Multinomial logistic regression: the result can have more than two possibilities.

In order to determine the value of probabilities, logistic regression uses the sigmoid function, which gives probabilities in values between 0 and 1. This function is defined as follows:

$$\boldsymbol{sig(X)} = \frac{\mathbf{1}}{\mathbf{1}+e^{-X}} \qquad (1.6)$$

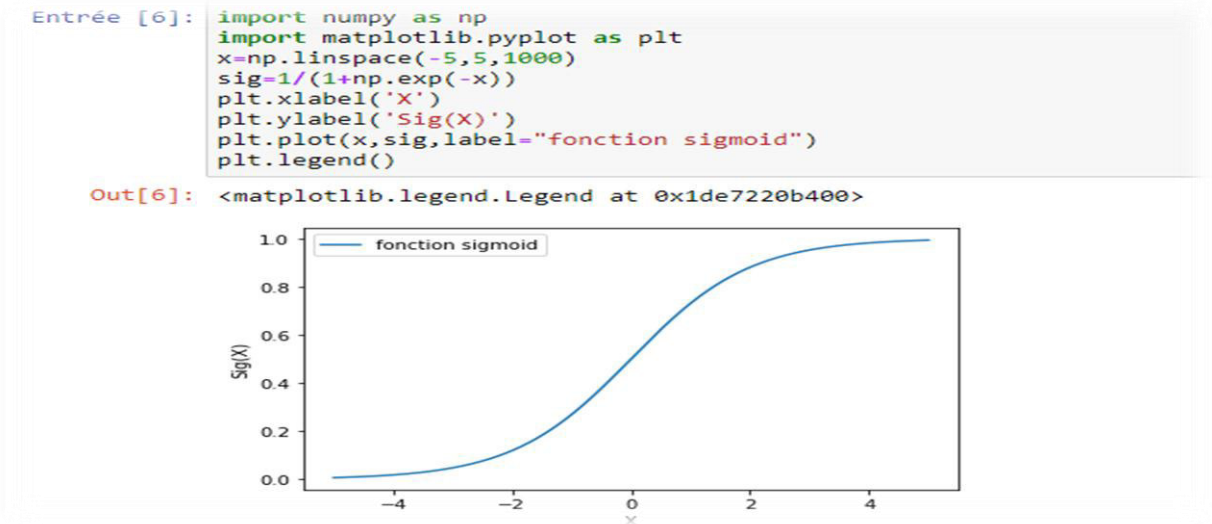

Figure 7: The sigmoid function in Python

1.4.1.2.2 Unsupervised learning:

This is a type of machine learning that has input data X and no output data Y, meaning there is no answer. This type of learning is used to divide data into groups or categories.

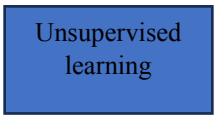

Figure 8: Example of unsupervised learning

It is called unsupervised because the algorithms are left to their own devices to discover and analyze the data.

Unsupervised learning is divided into two classes of algorithms:

Clustering algorithm.

Association algorithm.

1.4.1.2.2.1 Clustering algorithm:

Clustering is the process of separating or dividing data sets into several groups, in which data sets belonging to the same group are more similar to each other than to data sets in other groups.

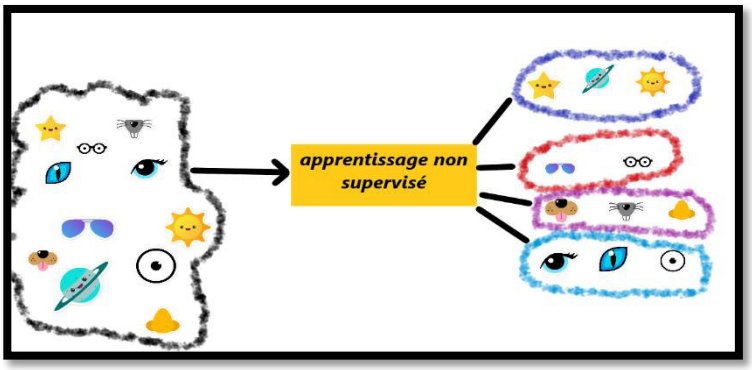

This method can be used to:

- Promote data visualization.
- Infer attributes from data.

1.4.1.2.2.1.1 K-Means:

This is a widely used iterative unsupervised learning algorithm that divides unlabeled data sets into different groups in which each data set belongs to only one group with similar attributes.

To apply the K-means algorithm:

Select the number of groups K and randomly select the centers of each group, then assign each point to the nearest center.

Calculate the distance between these points and the center of each group, then rank them according to the calculated distance and reassign the points to the new center closest to each cluster. Finally, we continue to randomly reconfigure the group centers until we obtain the cycle that gives the best result.

1.4.1.2.2.1.2 Principal Component Analysis (PCA or ACP):
This is an unsupervised learning algorithm that uses quantitative tabular data. PCA reduces the dimensions of the data and retains the greatest amount of information to obtain a new set of data called "Components," where the first component represents the largest variable in the data, while the second is the second largest variable, and so on.

First, you need to know the objective of the analysis and have a dataset containing the data. Next, try to center and reduce the variables (mean value = 0 and standard deviation = 1), then treat the data as an n-axis (n-dimensional) matrix and calculate the eigenvalues and eigenvectors, where the eigenvalues are used to determine the number of principal components.

1.4.1.2.2.2 Association algorithm:
This method allows you to sort and aggregate data related to specific characteristics in order to obtain things that are related to each other, provided that they are not identical. In short, it is a technique used to detect the possibility of a common element in the group.

1.4.1.2.3 Semi-supervised learning:
Semi-supervised learning, or transductive learning, is a neutral form of learning between supervised and unsupervised learning that uses both labeled and unlabeled data.

1.4.1.2.4 Reinforcement learning:

This is a type of machine learning that allows a machine to learn from its mistakes in order to make the right decisions in the future.

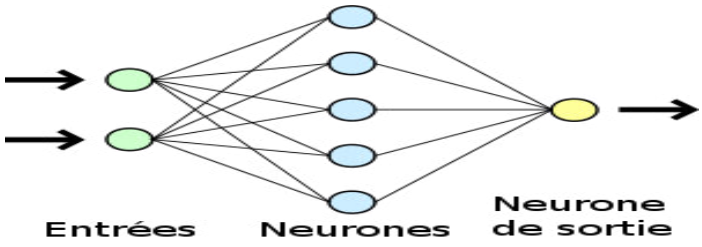

Reward status

Figure 9:

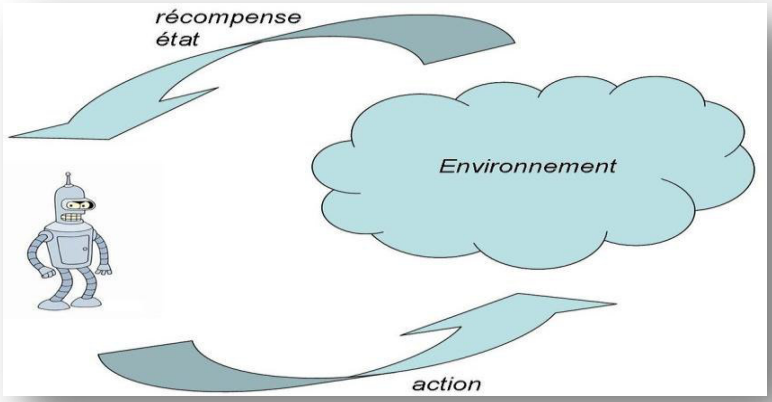

Reinforcement learning [5]

1.4.1.3 Deep learning (DL):

1.4.1.3.1 The neural network:

The neural network is a group of algorithms consisting of several layers of nodes connected to each other, enabling it to analyze huge amounts of data in a manner similar to the human brain.

Figure 10: Neural network [6]

1.4.1.3.1.1 Neural network architecture:

The neural network consists of three main layers:

- The input layer: reads incoming data.
- The hidden layer: This is an intermediate layer between the input layer and the output layer, where data is processed.
- The output layer: Provides the answer to the problem.

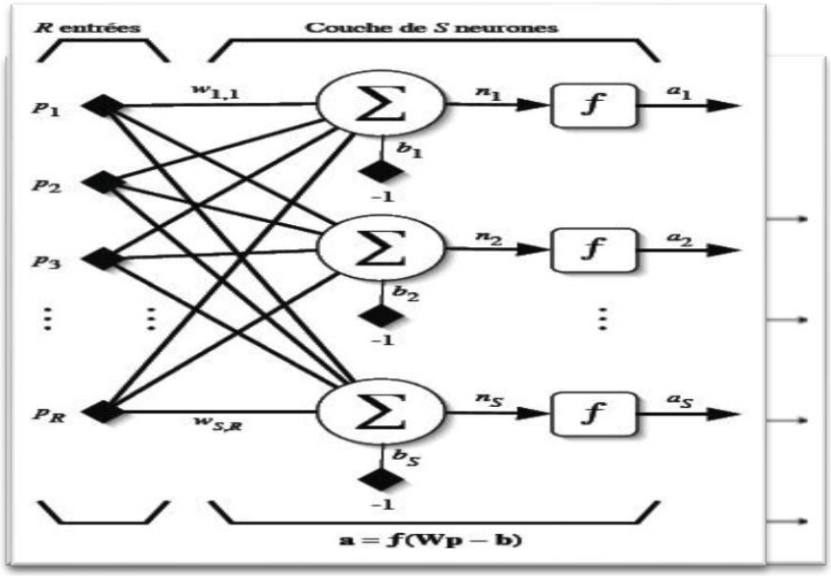

Figure 11: Neural network architecture [7]

1.4.1.3.1.2 How neural networks work:

Neural networks work in three steps:

i. Receiving information; this process takes place at the input layer.

ii. Weighted sum; this process takes place at the hidden layer.

iii. Response; this process takes place at the output layer.

An artificial neuron consists of a weight vector w, a bias b, and an activation function f.

It takes a vector p as input and returns the quantity f (∑ pi wi – b) as output. The activation function f generally mimics the electrical response (action potential) of a biological neuron. The neurons are then combined to form a layer that accepts the vector "p" as input and outputs the vector "a." Finally, the layers of neurons are connected to each other to form the final network.[8]

Figure 12: Model of a layer of artificial neurons [9]

1.4.1.3.1.3 The activation function:

The activation function, transfer function, or override function. This is a mathematical function that is generally non-linear (except in the case of the Relu function) and is applied to the hidden layers and output layer. It is used to capture the non-linearities present in the data.

For the neural network to perform well, the activation function for the hidden layer and even for the output layer must be chosen carefully.

1.4.1.3.1.3.1 The activation function for the hidden layer:

There are three activation functions suitable for the hidden layer (there are other functions, but these are the most appropriate and most common):

- The RELU function
- The sigmoid function
- The tanh function

The default activation function in modern neural networks is: the RELU function.

1.4.1.3.1.3.1.1 The RELU function:

The Relu function, or "rectified linear function," is the most commonly used function in hidden layers.

This function is defined by: max (0.0,X)

This means that if the input value (x) is negative, a value of 0.0 is returned, otherwise the value is returned. [10]

$$RELU=\begin{cases} \mathbf{0} & \boldsymbol{si}: \ \boldsymbol{x} < \mathbf{0} \\ \boldsymbol{x} & \boldsymbol{si}: \ \boldsymbol{x} \geq \mathbf{0} \end{cases} \qquad (\mathbf{1.7})$$

```
Entrée [24]: import numpy as np
             import matplotlib.pyplot as plt
             def RELU(x):
                 return max(0.0, x)
             X=np.linspace(-10,10,100)

             relu=[RELU(x) for x in X]
             plt.xlabel('X')
             plt.ylabel('Y')
             plt.plot(X,relu,label='LA FONCTION RELU')
             plt.legend()
Out[24]: <matplotlib.legend.Legend at 0x21638df30a0>
```

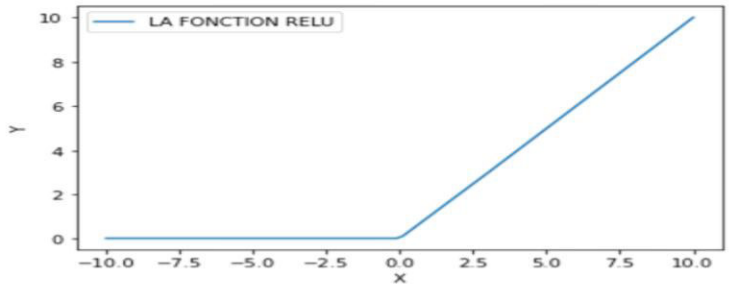

Figure 13: The RELU function in Python

1.4.1.3.1.3.1.2 The activation function for the output layer:

There are three activation functions suitable for the output layer (there are other functions, but these are the most appropriate and most common):

- The linear function
- The sigmoid function
- The softmax function

The activation function selected in the output layer depends on the type of problem to be predicted (classification or regression).

1.4.1.3.1.3.1.2.1 For the regression problem:

- For the linear regression problem, the linear function must be used.
- For the logistic regression problem, the sigmoid function must be used.

Table 2: The activation function in the regression problem

Types of regression:	**The activation function:**
Linear regression	linear
Logistic regression	Sigmoid

1.4.1.3.1.3.1.2.2 For the classification problem:

There are three types of classification problems.

Table 3: The activation function in the classification problem

Types of classifications:	The activation function:
Binary classification	Sigmoid
Multi-class classification	Soft-max
Multi-label classification	Sigmoid

1.4.1.3.1.4 The Cout function:
This function is used to minimize error and update weights. It compares the predicted value with the true value.

The Cout function is given by:

$$C = {}^{1}/_{2}\,(y - \hat{y})^{2} \qquad (1.8)$$

1.4.1.3.1.5 Weight:
Weight is the link between units. The weight space is a parameter that converts input data into output by multiplying it by the weight. It then transfers the processed data to other neurons in artificial neural networks via the output layer. [11]

1.4.1.3.1.6 Types of neural networks:
There are several types of neural networks, the most famous of which are:

1.4.1.3.1.6.1 Recurrent neural network (RNN):
A recurrent neural network is a type of neural network in which information can propagate in both directions [12]. This network is suitable for input data of different sizes and is particularly well suited to time series analysis. However, recurrent neural networks encounter the problem of gradient disappearance when learning to remember past events.

1.4.1.3.1.6.2 Convolutional neural network (CNN):
A convolutional neural network is a type of multilayer neural network specialized in image processing. CNNs use convolution in at least one of their layers instead of regular matrix multiplication.

1.4.1.3.1.6.3 Restricted Boltzmann machine (RBM):
A restricted Boltzmann machine is a type of neural network for unsupervised learning. It is commonly used to estimate the probabilistic distribution of a dataset. It was originally invented under the name Harmonium in 1986 by Paul Smolenski. [13] It was adapted from statistical physics for use in cognitive science. The Boltzmann machine is based on a stochastic spin glass model with an external field [14]. This network consists of two layers: "an input layer and a hidden layer."

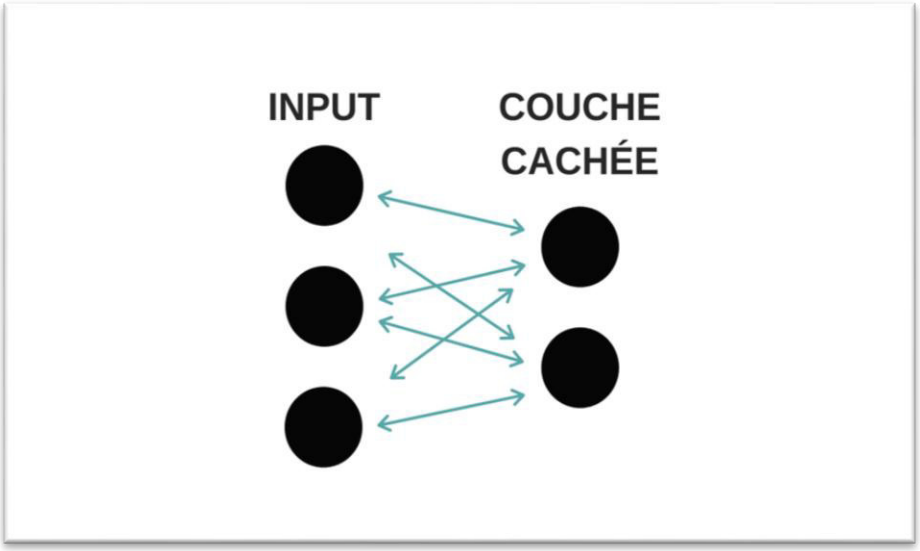

Figure 12: The restricted Boltzmann machine [15]

1.4.1.4 Conclusion:

In this part , we discussed machine learning and deep learning in general terms. We then presented some ML and DL algorithms.

1.4.2 current application of AI in medical physics and radiotherapy:

1.4.2.1 AI for target and organ segmentation :

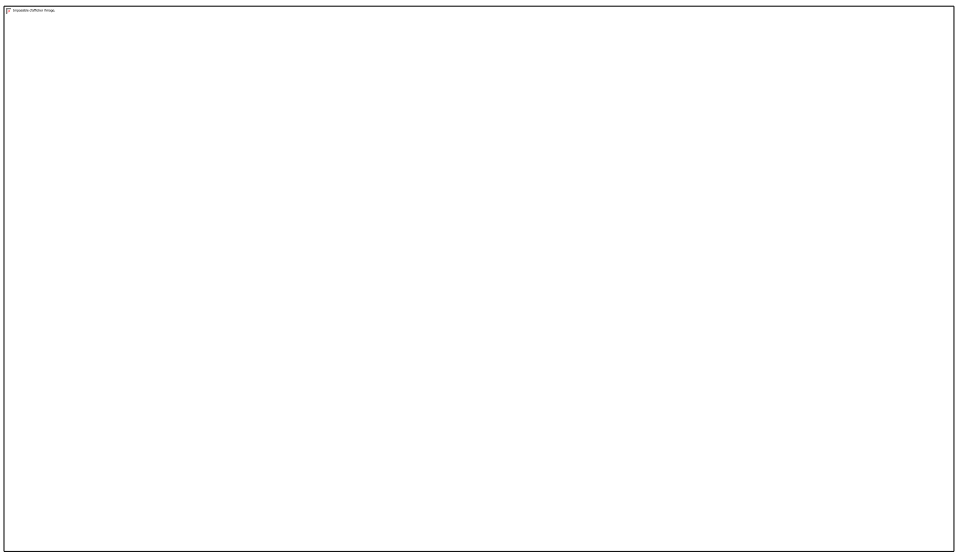

Radiation oncologists have an important role in determining the volume of tumor targets (GTV) . However, medical images can sometimes being unclear or blurred, making it difficult to seperate between normal and tumor tissues. (3). Identifying organs at risks (OARs) is also time-consuming. AI-based methods, especially deep learning, have improved tumor and OARs segmentation in CT, MRI, and PET scans. However, their are challenges such as the need for large, well-annotated datasets and integrating multiple imaging sources for better accuracy. [1, 2]

1.4.2.2 AI for image registration :

Image registration is widely used in clinics for tasks like motion tracking, segmentation, and adaptive radiation therapy (4, 5, 6). However, traditional methods, especially deformable image registration (DIR), can take hours due to iterative optimization. (7) AI-assisted registration significantly speeds up the process with a single forward calculation. (8) AI models fall into three types: deep iterative, supervised, and unsupervised registration. While AI improves accuracy and efficiency, challenges remain, such as limited high-quality training data and ensuring realistic deformations.(9) Further research is needed to refine AI-based registration methods for clinical use.

1.4.2.3 Deep learning-based image reconstruction:

One of the modern techniques that has proven it effectiveness is enhancing the quality of medical image reconstruction, such as CT, MRI and PET. DL is characterized by its ability to extract complex features that are difficult for traditional method to detect, allowing for improved image accuracy and a reduction in artifacts associated with conventional reconstruction techniques. [10]

Among the notable models, AUTOMAP was developed for image reconstruction from k-space data. [10] Additionally, DL has enabled a reduction in the amount of data required for medical image reconstruction without compromising quality, by leveraging prior patient data to enhance imaging accuracy and reduce the need for additional measurements. [12]

1.4.2.4 AI for dose prediction and automated treatment planning:

the revolution in radiation therapy, means using of AI in automation and optimizing treatment planning, Current planning relies heavily on manual trial-and-error, leading to variability in treatment quality. [11] AI-augmented approaches, particularly deep learning, offer solutions for dose prediction incorporating anatomical and dosimetric features, automated parameter adjustments, and faster dose calculations. [13-18] This would improve efficiency, treatment plan quality, and standardization. [11] However, challenges remain, including the need for models to better balance tumor dose maximization with organ damage minimization, incorporate delivery parameters beyond dose maps, and clinically implement AI based dose prediction with prior clinical knowledge. [19,20]

1.4.2.5 Deep learning-augmented image guidance:

Deep learning plays an immensely important role in supporting image guidance in radiation therapy for the accurate targeting of the beam, especially in advanced techniques like VMAT,

IMRT, SRS, and SABR, which demand a high level of positional targeting [11]. Deep learning allows greater operation for image-guided radiation therapy (IGRT) by learning complex relations from data [13], for example, the markerless and highly accurate localization of the prostate using kV X-ray images with an accuracy of fewer than 1mm has been done [14, 15, 16]. Likewise, advanced AI applications have come in handy in motion management [17] and quality assurance [18] of radiation therapy, with strict adherence to real-time target tracking of 500ms latency [19]. But, even as isolated instances reveal commendable results for individual components, meaningful prospective studies must be conducted to understand possible latencies across the entire treatment pathway, including image reconstruction and data transfers.[11]

1.4.2.6 Deep learning-based outcome prediction:

Deep learning in radiation therapy generates ever-increasing interest in outcome predictions, thereby showing its worthiness in several applications. Apart from predicting patient survival and local progression after stereotactic body radiation therapy utilizing 3D dose analysis, others are developments of deep learning models that build toxicity risk maps and predict long-term death rates for tumors such as colorectal cancer with high accuracy based on tumor features, medical history, and demographic information. Apart from these, patient-based deep learning models built from comprehensive dose-volume histogram data are being developed to predict complications such as lymphopenia, thereby allowing more granularity than traditional methods utilizing simple indices. With increasing access to high-quality clinical data and advanced methods in deep learning, the development of clinically relevant predictive models will greatly accelerate.[21-25]

Figure 5 : Potential applications of artificial intelligence in medical physics and radiotherapy

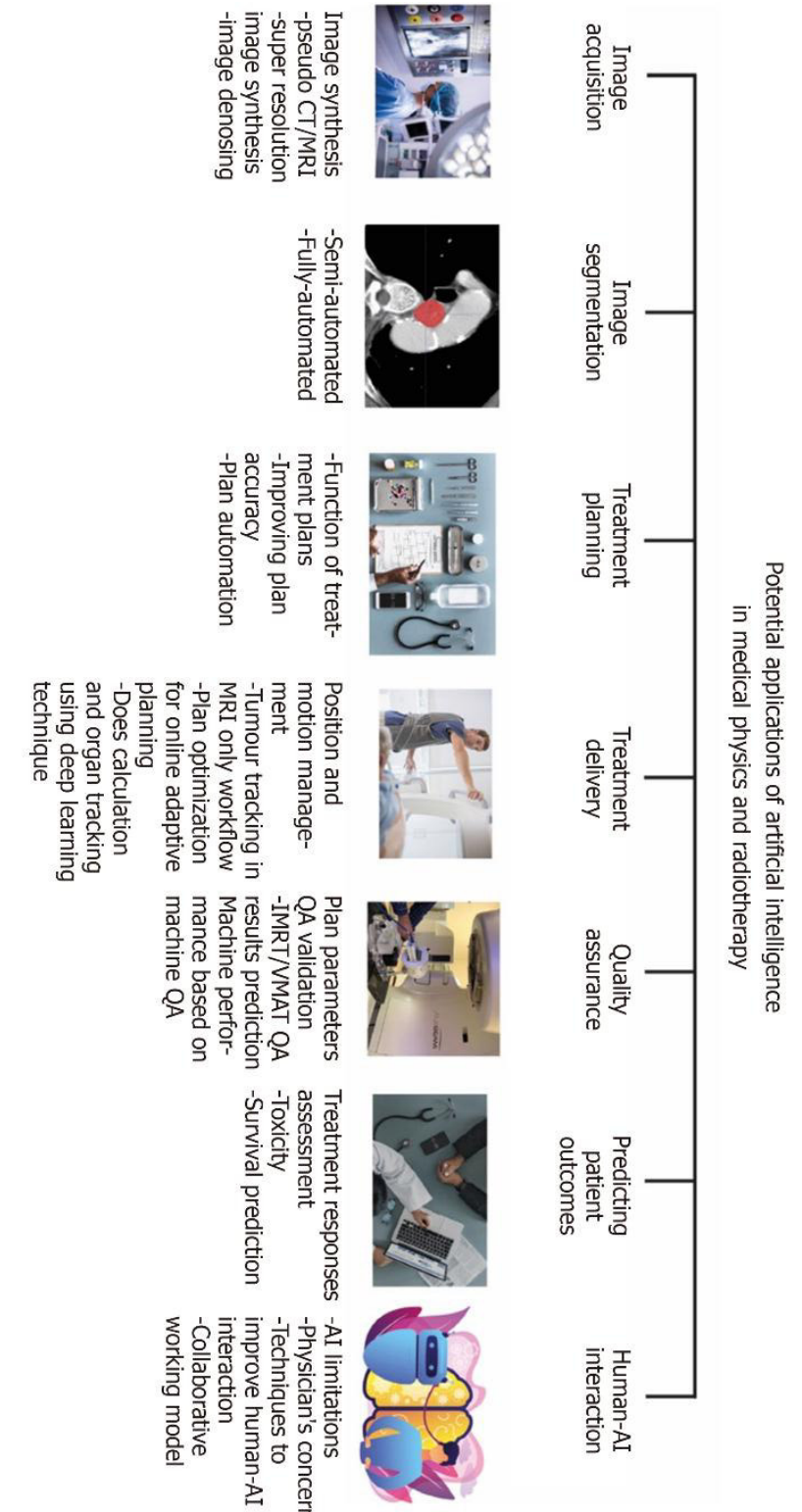

1.4.3 comparison with traditional methods:

Aspect	**Traditional**	**AI-Based**	**Supporting References**
Medical Imaging	Manual image acquisition and interpretation relying on human expertise; standard reconstruction algorithms.	AI enhances image quality, automates segmentation, improves detection and classification accuracy, and speeds diagnosis.	[2], [4], [7], [8]
Treatment Planning	Time-consuming manual or semi-automated planning; relies on physicist's experience for dose calculations and optimization.	AI automates and streamlines treatment planning, optimizing dose distribution rapidly and reducing planning time.	[2], [4], [5]
Diagnostics	Diagnosis based on physician interpretation and conventional statistical analysis.	AI uses deep learning to detect subtle patterns, improving diagnostic accuracy and early disease detection.	[4], [5], [8]
Workflow Efficiency	Manual workflows with potential for human error and delays.	AI-driven automation reduces workload, minimizes errors, and provides real-time decision support.	[4], [5], [6]
Personalized Treatment	Treatment protocols based on population averages and clinical guidelines.	AI enables precision medicine by tailoring treatment plans to individual patient data and response patterns.	[5], [4]
Quality Assurance	Periodic manual checks and calibrations of equipment; resource-intensive.	AI supports continuous monitoring, anomaly detection, and predictive maintenance to enhance QA processes.	[1], [7]
Data Handling & Analysis	Limited by manual data processing and traditional statistics.	AI leverages big data and advanced analytics for improved pattern recognition and predictive modeling.	[1], [4], [8]
Challenges	Limited by human variability, slower processing, and less adaptability.	Requires large datasets, transparency (explainability), data privacy safeguards, and integration into clinical practice.	[1], [4], [5], [7]

1.5 Conclusion:

This chapter carried the evolution of radiation therapy:

- From Rontgen's discovery of X-rays , and beams therapy to contemporary technologies such as IMRT, IGRT, and proton therapy.
- Also highlighted the behavior of radiation beams , like understanding their properties , the factors influcing their interaction with matter , and the paramount importance of accurate beam modeling in treatment planning. This modeling, enhanced by Monte Carlo simulations and rigorous TPS commissioning, ensures precise dose delivery, customization for various treatment modalities, and ultimately, improved patient safety.
- and addressed the potential benefits of utilizing artificial intelligence in the future of medical physics and radiotherapy. Artificial intelligence, which includes subsets of machine learning, deep learning, and automation, has many possible benefits across many applications. These include improving the accuracy and efficiency of targeting and organ segmentation during imaging, image registration, enhancing dose prediction models, incorporating automation with treatment planning, and image guidance enhanced with deep learning. With the use of deep learning, there is a potential for AI to play a role in predicting patient outcome information too, which can then be used as information in creating personalized treatment plans.

CHAPTER TWO

2 Literature Review

2.1 Introduction to the literature review:

2.1.1 Purpose and scope:

This chapter aims to provide a comprehensive review of the current literature on the application of artificial intelligence (AI) in radiotherapy beam modelling the scope of this review includes studies investigating the use of AI techniques for various aspects of beam modeling, including dose prediction, beam parameter optimization and quality assurance. given the critical role of accurate beam modeling ensuring the efficacy and safety of radiotherapy, this review will analyze how AI methods can enhance and improve current practices.

2.1.2 Search strategy and methodology:

The literature search was conducted using electronic databases such as IEEE Xplore, ResearchGate, Journal of Radiation research, PubMed central, Science Direct and physicamedica. The search strategy included a combination of keywords and medical standardized terms (MeSH) such as: “artificial intelligence “ , “Machine learning “ , “ Deep learning “ , “ radiation therapy “ , “ beam modeling “, “dose prediction “,” dose distribution “, “treatment planning “ . The inclusion criteria were limited to peer-reviewed articles published in English and official websites.

2.2 AI techniques in radiation beam modeling:

2.2.1 AI for dose prediction:

Accurate dose prediction is important in radiation therapy planning, to ensure that the planned dose is accurately delivered to the target volume (GTV) while minimizing exposure to organs at risk. Traditional methods often involve complex calculations and may be limited in heterogeneous media or complex geometries. Artificial intelligence (AI) techniques, especially machine learning and deep learning, are promising for improving the accuracy and efficiency of dose prediction.

Chen et al. presented a systematic approach to optimize beam models to achieve dosage accuracy across a wide range of treatment conditions. They emphasized the importance of testing dose calculation algorithms under diverse clinical scenarios to ensure prediction accuracy. This work highlights the complexities of beam modeling and the need for robust validation methods, which AI can address.

The American Association of Medical Physics (AAPM) Working Group 157 report provides a comprehensive review of beam modeling and commissioning of Monte Carlo dosimetry-based treatment planning systems. Monte Carlo methods are known for their high accuracy in dose calculation, but the report also discusses the complexities of beam modeling and the need for accurate commissioning to ensure accuracy. AI techniques can simplify and improve the efficiency of Monte Carlo processes, or provide accurate and fast alternatives.

2.2.2 AI for optimization of beam parameters:

Optimization of beam parameters, such as angles and intensities, is important to achieve dose distributions with high conformity to the target without damaging the organs at risk. Artificial intelligence has been explored to automate and optimize this process.

Kawamura et al. reviewed the promises of AI in radiation therapy, for example, in treatment planning and optimization. They stated that AI can significantly reduce the time in treatment planning, which can improve the efficiency of the workflow in radiation therapy overall. AI algorithms can interpret complex datasets and detect optimal beam parameters, which may be difficult to detect using traditional methods.

2.2.3 AI for beam delivery quality assurance:

Precise and stable delivery of radiation beams is of utmost importance for patient safety and treatment outcome. Artificial intelligence can be utilized to analyze beam data, detect deviations from the treatment plan, and even foresee errors.

Landry et al. discussed broader applications of AI in radiation therapy, including its application in quality assurance. AI can be used to track the parameters of treatment delivery and identify potential discrepancies making the treatment process more reliable and effective.

2.3 Challenges and Limits:

2.3.1 Data Requirements:

One of the biggest challenges to the use of AI for beam modeling is the need for large, high-quality datasets. AI models, especially deep learning models, require large datasets to successfully train them and enable them to generalize to new situations. In radiotherapy, the collection of data may be complicated by the variety of treatment methods, patient anatomy, and equipment that may be utilized. Landry et al. highlighted the need for data collection in radiotherapy and the challenge of generalizing the results.

2.3.2 Generalization and validation of models:

It is essential to make sure that models generalize to new and different data in clinical practice. Overfitting, where models perform well with training data but poorly with new data, is a common issue Rigorous validation needs to be employed to assess the robustness and reliability of AI models in beam modeling.

Chen et al. have emphasized the necessity to validate models under a wide range of conditions to ensure empirical accuracy.

2.3.3 Explainability and Transparency:

The majority of AI models, especially deep learning models, are "black boxes", and it is difficult to interpret how they arrive at decisions. In a clinical setting, interpretability is required to earn the trust of AI-based beam modeling tools among clinicians. They need to understand the reasoning of AI predictions to make clinically appropriate decisions.

2.3.4 Clinical application and workflow integration:

One more issue is the compatibility of the integration of AI-based beam modeling and treatment planning with existing clinical systems. Issues about data compatibility, software integration, and usability through the availability of user-friendly interfaces must be addressed to enable clinical implementation of AI.

2.4 Research gaps and rationale:

2.4.1 Overview of the main findings:

The literature reviewed indicates the great potential of AI to improve different aspects of radiotherapy beam modeling, such as dose prediction, beam parameter optimization, and quality assurance. Different studies have shown that dose calculation efficiency and accuracy can be improved by AI algorithms, the automation of beam parameter optimization, and the enhancement of quality assurance procedures. These advancements are yielding more accurate and detailed treatment plans. Challenges remain, however, in data demands, model generalizability across different patient anatomies, interpretability of AI decisions, and their integration into clinical workflows effectively.

2.4.2 Identification of research gaps:

Although the advances in AI technologies for radiotherapy are notable, there are a few important research gaps to be filled:

- Accurate dose prediction in anatomically complex regions: Current models are likely to fail at accurate prediction of the dose distribution in heterogeneous tissue and anatomically complex regions. AI models should be created that can overcome such limitations and increase the accuracy of predictions under such conditions.

- Beam parameter optimization for multiple clinical targets: Current optimization techniques generally focus on a single clinical target. There is a need for AI models that can optimize for multiple clinical targets simultaneously, like target coverage and minimizing sensitive organ exposure.

- Interpretability and transparency of AI models: Deep learning models often function as "black boxes," making their results difficult to interpret, and this can affect the confidence of clinicians. Interpretable models need to be developed that allow experts to understand the rationale behind the predictions and take decisions accordingly.

- Seamless integration with existing treatment planning systems: AI software must be designed to integrate seamlessly into existing treatment

planning and clinical workflows planning and treatment systems without disruption, helping treatment teams make accurate decisions without the need for drastic workflow changes.

2.4.3 Research Motivation and Significance:

The motivation of this research is to build an artificial intelligence model based on existing data that helps physicians make accurate and informed decisions when selecting radiation therapy plans for cavum cancer patients. The research focuses on reviewing recommendations for radiation dose to critical organs, monitoring the compliance of the planned dose with these recommendations, and issuing alerts if the dose exceeds the permissible limits.which enhances the assessment of the effectiveness and quality of the treatment plan.

This model aims to improve decision-making efficiency and reduce errors associated, which positively impacts the quality and safety of treatment.

CHAPTER THREE

3 Chapter 03: data collection and results:

3.1 Data collection and preprocessing:

3.1.1 Data sources and number of cases:

The data used in this work was collected from the center of anti cancer – Tlemcen, after obtaining prior approval and ensuring patient anonymity, this clinical data enhances the credibility of the model. The database includes 10 patients in cavum cancer.

3.1.2 Nature of extracted Data and Preparation:

The collected data includes technical information and treatment doses, extracted from the Eclipse /Aria treatment planning system and comprises:

- DVH (Dose Volume Histogram) information for each patient and plan.
- Information on Organs at risk (OARs) for each treatment plan.
- Doses : Maximum dose (Dmax) Mean dose (Dmean) , Minimum dose (Dmin) , and Prescribed dose .
- Plan distribution: some patients have one plan, while others have two or three plans .

All data was arranged in a CSV file and organized to be suitable for training an artificial intelligence model.

3.1.3 Organs At Risk and Their Classification:

In case of cavum cancer , the following critical organs are identified : spinal cord , brain , brainstem , Lens , eyes , optic nerves , parotid and inner ears , these organs are classified according to their sensitivity to radiation :

Serial organs, such as the spinal cord and brain.

Parallel organs, such as the parotid glands and larynx.

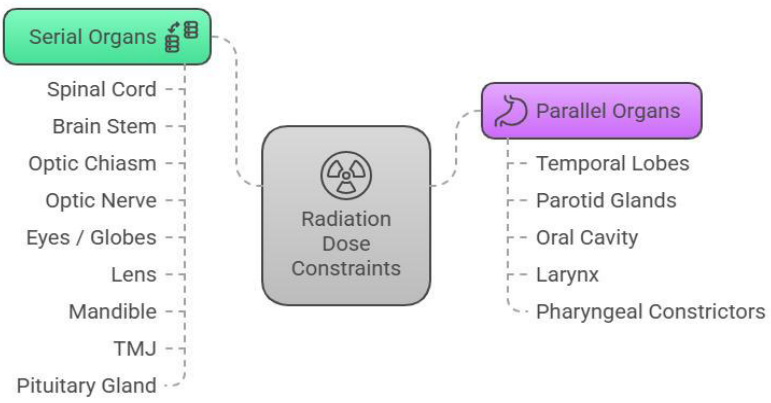

Figure 01 : Organ At Risk (OAR) classification for Radiotherapy Planning

The permissible dose limits have been adopted based on recommendations approved in scientific literature, such as:

1. S. Bisello, S. Cilla, A. Benini, *et al*., Dose–Volume Constraints for Organs at Risk in Radiotherapy (CORSAIR): A Practical Multicenter and Multidisciplinary Summary *Curr. Oncol.*, vol. 29, pp. 7021–7050, 2022, doi: 10.3390/curroncol29100552.
2. P. Xia, "Optimization for IMRT (I) – Fundamental Issues," presented at *AAPM Annual Meeting*, San Francisco, CA, USA, 2005, Course MO-B-T-6E, Univ. of California–San Francisco.

The values extracted from each treatment plan were included in the database, including the maximum dose (Dmax), mean dose (Dmean), and minimum dose (Dmin) for each organ, along with an assessment of whether the treatment constraints for each organ were respected (Eval_plan_OAR).

Organ	Type	Dose Constraint
Spinal Cord	Serial	Dmax < 45 Gy
Brain Stem	Serial	Dmax < 54 Gy
Optic Chiasm	Serial	Dmax < 54 Gy
Optic Nerve	Serial	Dmax < 54 Gy
Eyes / Globes	Serial	Dmax < 45 Gy
Lens	Serial	Dmax < 6 Gy
Parotid Glands	Parallel	Mean < 25 Gy (both), V30 < 50%
Mandible	Serial	D20% < 65 Gy, Dmax < 70 Gy
Oral Cavity	Parallel	V30 < 73%, limit mean dose
Larynx	Parallel	Mean < 50 Gy, V50 < 27%, Dmax < 73.5 Gy

Table 01 : Organ At Risk (OAR) Dose Constraints for Radiotherapy Planning

3.2 Database description :

This chapter provides a detailed interpretation of this study's results focusing the developed prediction model and its performance using the PyCaret library [1].

The main goal was to build a classifier that could assess OAR risk levels under radiotherapy planning procedures. By investigating the clinical data, including radiation doses and anatomical structures the classifier assigns each structure to one of four risk categories: Safe, Medium Risk, High Risk, or Unknown.

The dataset contains 228 records in 19 features, with a careful preprocessing stage to remove bias introduced by class imbalance and to ensure that the resultant output is reliable. Multiple machine-learning models were applied and assessed, with the CatBoost Classifier showing maximum performance with respect to accuracy, recall, precision, and F1 score.

This chapter presents the core findings, including feature importance, classification reports, confusion matrix results, and ROC curve analysis, underscoring the ability of the model to very accurately classify cases as high risk, which is a prime requisite in medical decision-making.

3.3 Data Visualization:

Figure 3: OAR Evaluation Distribution per Structure

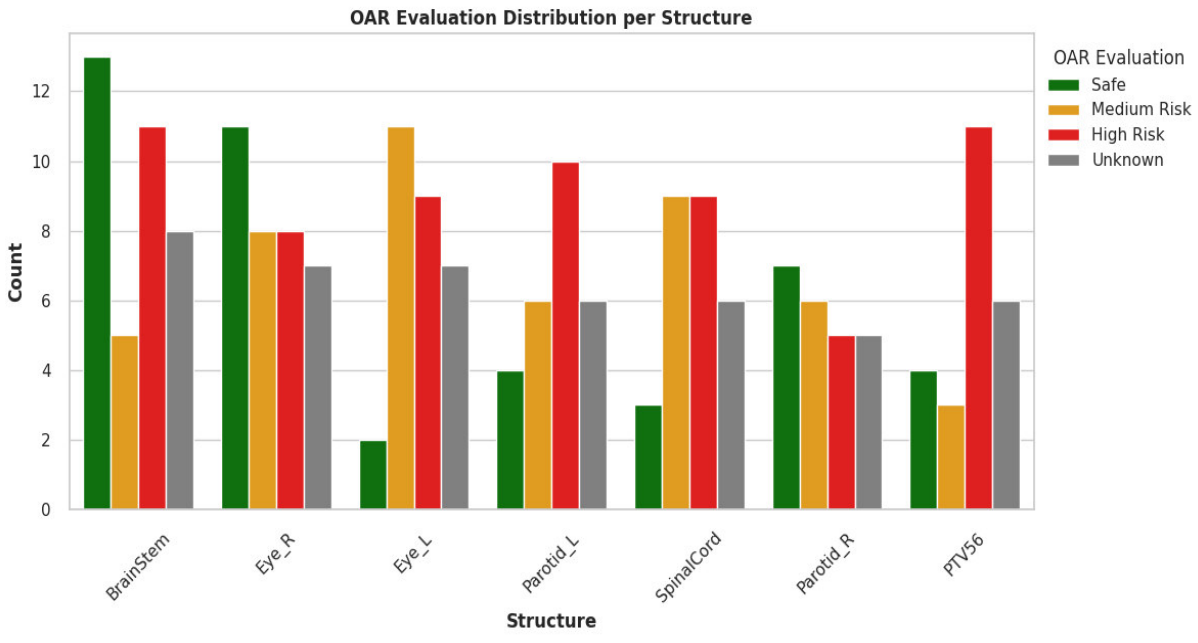

Objective of the Figure:

Figure 1 is a bar chart that illustrates the distribution of Organ At Risk (OAR) evaluations across different anatomical structures, categorized by four risk levels:

- Safe: Structures deemed safe from excessive radiation exposure.

- Medium Risk: Structures with moderate risk of adverse effects due to radiation.

- High Risk: Structures highly susceptible to significant damage from radiation.

- Unknown: Structures where the risk level is unknown data is available.

This helps to identify which anatomical structures are more frequently classified into each risk category, providing insights into the relative safety or danger associated with various organs during radiotherapy treatment planning

remarkable Observations from the Figure:

1. Structures Frequently Categorized as "Safe":

- Brainstem, Right Eye (Eye_R), and Right Parotid (Parotid_R) show a high balance of cases classified as Safe.

For example:

- The Brainstem has the highest number of Safe as 13 cases , indicating that this structure is often considered safe in the context of the analyzed dataset.

- Similarly, the Right Eye and Right Parotid also have a substantial number of Safe classifications, suggesting that these structures are less likely to be exposed to harmful doses of radiation in most treatment plans.

2. Structures at Higher Risk:

- Left Eye (Eye_L), Left Parotid (Parotid_L), and Spinal Cord (SpinalCord) are particularly classified as High Risk.

- Key remarks:

- The left eye presents a significantly greater number of high-risk cases in comparison with all other structures. This would indicate a high dose of radiation was administered to the left eye or that the anatomy of the left eye is predisposed to be more affected based on the tumor location .

- The left parotid gland presents very many high-risk cases, indicating that this structure is often exposed to potentially harmful levels of radiation.

- The spinal cord is yet another structure with a good number of high-risk cases, reflecting the degree of its sensitivity to radiation and the infeasibility of protecting it adequately throughout treatment. - There is a noticeable asymmetry between left-side and right-side structures:

- Right-side structures (e.g., Right Eye, Right Parotid) are more frequently classified as Safe.

- Left-side structures (e.g., Left Eye, Left Parotid) are more frequently classified as High Risk.

Explanations:

- Treatment planning could probably weigh the importance of shielding the right side of the body more heavily, perhaps because of the tumor site or patient anatomy.

- Perhaps the left side is closer to the tumor, and hence radiation doses to those areas are higher. 4. Other Notable Observations:

- PTV_56: This structure (likely a Planning Target Volume receiving 56 Gy of radiation) shows a high number of High-risk cases, which is expected since it is the primary target for radiation therapy. However, it also has a significant number of Safe cases, indicating variability in treatment planning strategies.

- Unknown Category: Several structures, including the Brainstem, Right Eye, and Right Parotid, have cases classified as Unknown. This suggests that there may be uncertainty in assessing the risk level for these structures in some instances.

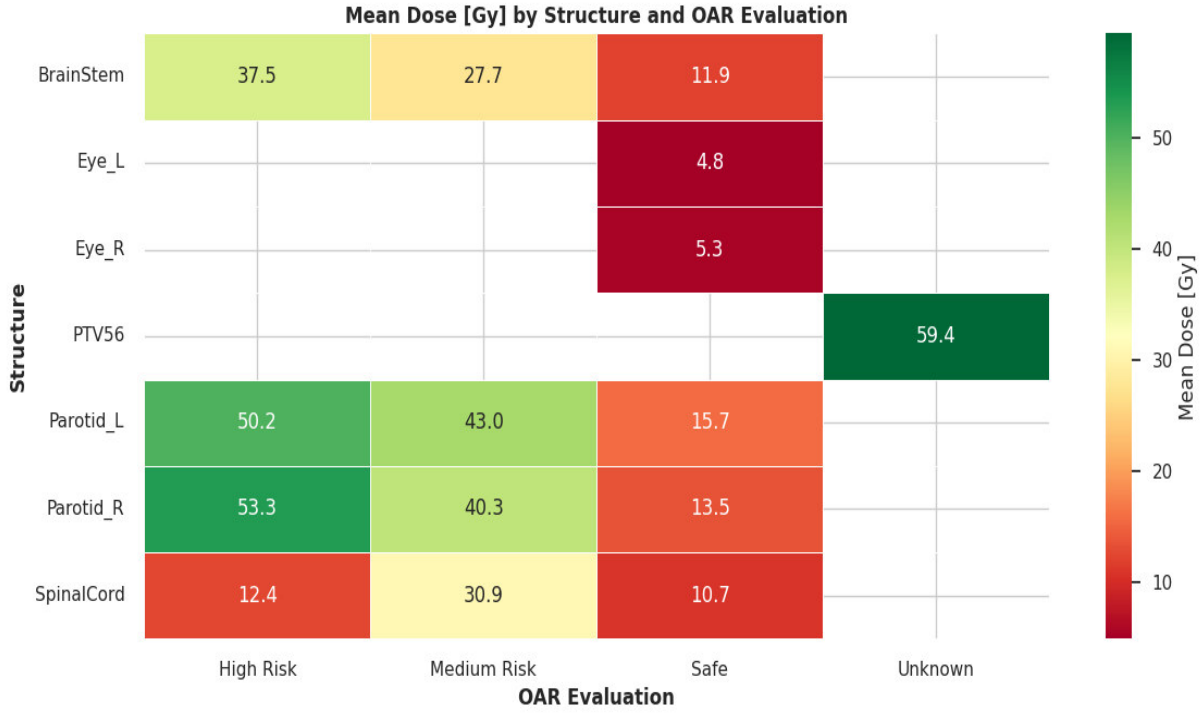

Figure 4: Mean Dose [Gy] by Structure and OAR Evaluation.

Figure 2 is a heatmap that visualizes the mean radiation dose (in Gy) received by different anatomical structures (OARs) across four riisk categories.

The goal is to understand how mean doses vary depending on both the anatomical structure and its risk level. This helps identify patterns in dose distribution and assess whether lower doses are indeed associated with lower risk levels.

remarkable Observations about the Heatmap:

1. General Trend: Lower Doses Correlate with Lower Risk Levels

As observed, lower average doses are consistently associated with lower risk levels.

Structures classified as Safe generally have the lowest mean doses.

Structures classified as High Risk or Medium Risk have higher mean doses.

The Unknown category shows variability but often includes higher doses.

2. Dose Distribution Across Anatomical Structures:

Different anatomical structures exhibit varying dose responses based on their risk classification:

STRUCTURE	SAFE	MEDIUM RISK	HIGH RISK
BRAINSTEM	11.9 Gy	27.7 Gy	37.5 Gy
EYE_L (LEFT EYE)			4.8 Gy
EYE_R (RIGHT EYE)	5.3 Gy		
PAROTID_L (LEFT PAROTID)	15.7 Gy	43.0 Gy	50.2 Gy
PAROTID_R (RIGHT PAROTID)	13.5 Gy	40.3 Gy	53.3 Gy
SPINAL CORD	10.7 Gy	30.9 Gy	12.4 Gy

Table 01 : Dose Distribution Across Anatomical Structures showing risk classification

The heatmap confirms the expected relationship: as the average dose decreases, the risk level also decreases.

This aligns with clinical guidelines that emphasize minimizing radiation exposure to critical organs to reduce adverse effects.

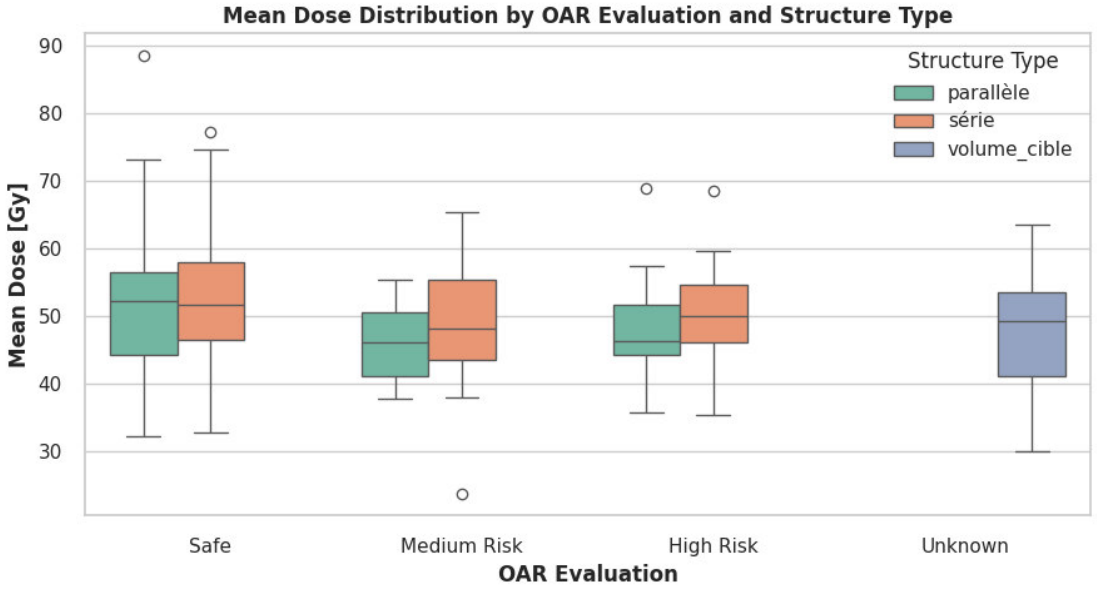

Figure 03 : Mean Dose Distribution by OAR Evaluation and Structure Type

figure is a boxplot that illustrates the distribution of Mean Dose (in Gy) across different OAR Evaluations (Safe, Medium Risk, High Risk, Unknown) for three types of structures: parallel , Serie, and volume_cible. The boxplot provides insights into how mean doses vary depending on the risk level and structure type.

1. Overall Distribution Across Risk Levels:

- The Mean Dose generally increases as the risk level increases:
  - Safe: Lower mean doses (around 40–50 Gy).
  - Medium Risk: Slightly higher mean doses (around 45–60 Gy).
  - High Risk: Higher mean doses (around 45–60 Gy).
  - Unknown: Highest mean doses (around 35–60 Gy).

This trend aligns with the expectation that higher doses are associated with higher risk levels.

2. Comparison Across Structure Types:

Dose Comparison by Structure Type and Risk

Characteristic	Parallel	Serial	Volume Cible
Mean Dose	Lower	Moderate	Highest
Safe Median Dose	~45 Gy	~55 Gy	~50 Gy
Medium Risk Median Dose		~55 Gy	~55 Gy
High Risk Median Dose	~50 Gy	~55 Gy	~55 Gy
Unknown Median Dose	Slightly higher, relatively low	~55 Gy	~55 Gy

Table 02 : Dose comparison by structure and risk

3.4 Data Preprocessing :

This step is crucial before starting prediction, where we filter our database, encode categorical variables, testing if the target variable is balanced across classes:

3.4.1 Check class Balance:

To evaluate whether the target variable ("OAR Evaluation") was balanced, we examined the distribution of its classes before modeling began.

If all classes have roughly equal representation, the dataset is said to be balanced. An imbalance in one or more classes creates bias in predictions. It was clear that the "Safe" class dominated the dataset as it constituted more than half of the observations. This imbalance could cause the model to predict "Safe" more often than not, adversely affecting its ability to effectively identify risky structures. This is a crucial aspect in medical applications.

Solution:

Applying Random Over Sampler: To address this imbalance, we applied the Random Over Sampler technique. This method artificially increases the number of samples in minority classes by duplicating existing instances until all classes are equally represented.

	BEFORE COUNT	AFTER COUNT	BEFORE %	AFTER %
OAR EVALUATION				

HIGH RISK	33	124	14.5	25.0
MEDIUM RISK	26	124	11.4	25.0
SAFE	124	124	54.4	25.0
UNKNOWN	45	124	19.7	25.0

Table 03: Relative Class Distribution (Before vs After Balancing)

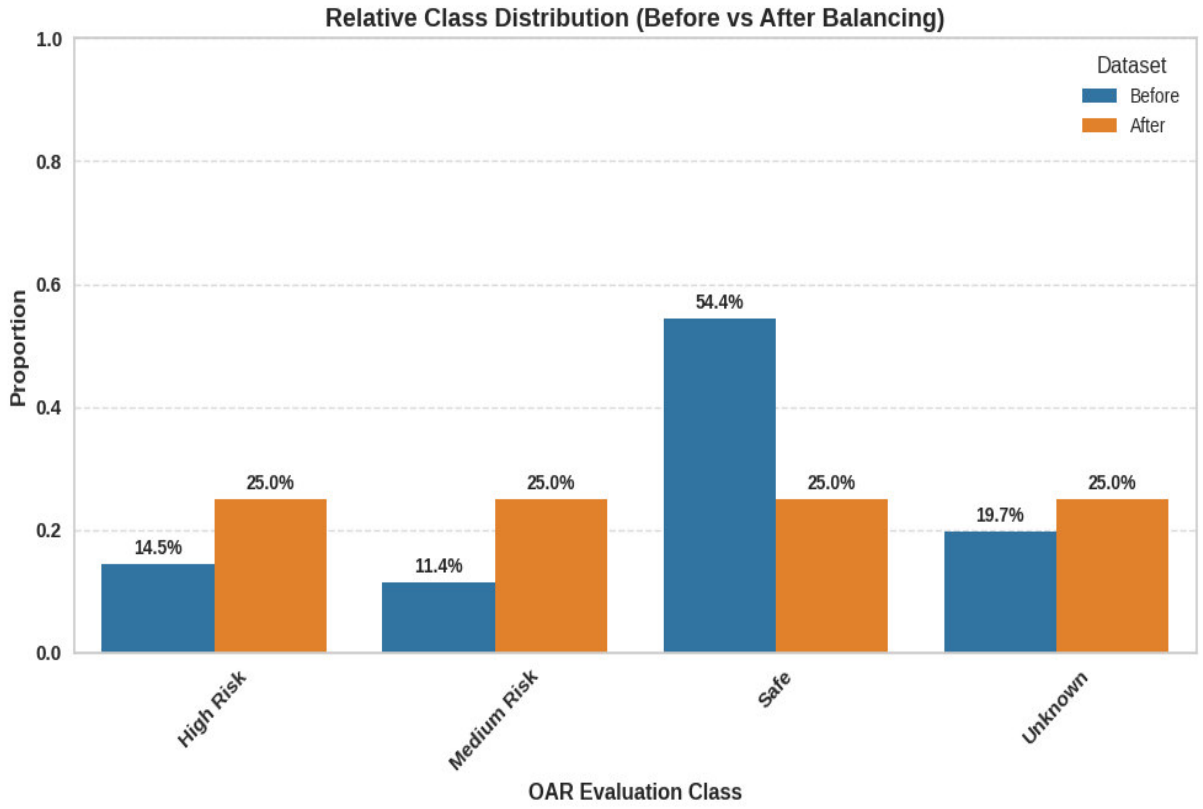

Figure 4: Relative Class Distribution (Before vs After Balancing)

3.5 Splitting the Data into Training and Testing Sets

For objective evaluation of model performance, the dataset was divided into subsets:

- 80% for training the model
- 20% for testing the model

This split allows us to train the model on a portion of the data and test it on unseen data to assess generalization capability.

3.6 Initializing Pycaret and Model Comparison

We used Pycaret [1], a low-code machine learning library, to initialize the environment and compare multiple classification models to identify the best-performing one.

Table 04: Compare model matrix.

3.6.1 Explanation of Classification matrix:

- **Accuracy:** Accuracy simply measures how often the classifier correctly predicts. We can define accuracy as the ratio of the number of correct predictions and the total number of predictions.[2]
- **AUC (Area Under the ROC Curve):** is the measure of the ability of a classifier to distinguish between classes.[2]
- **Recall (Sensitivity):** It explains how many of the actual positive cases we were able to predict correctly with our model.
  Recall is a useful metric in cases where False Negative is of higher concern than False Positive. It is **important in medical cases** where it doesn't matter whether we raise a false alarm but the actual positive cases should not go undetected.[2]
- **Precision:** It explains how many of the correctly predicted cases actually turned out to be positive.[2]

	Model	Accuracy	AUC	Recall	Prec.	F1	Kappa	MCC	TT (Sec)
catboost	CatBoost Classifier	0.9714	0.9976	0.9714	0.9752	0.9705	0.9619	0.9636	6.3320
gbc	Gradient Boosting Classifier	0.9643	0.0000	0.9643	0.9721	0.9639	0.9524	0.9552	0.8290
rf	Random Forest Classifier	0.9640	0.9988	0.9640	0.9700	0.9634	0.9520	0.9544	0.3110
et	Extra Trees Classifier	0.9566	0.9983	0.9566	0.9651	0.9558	0.9422	0.9455	0.3030
xgboost	Extreme Gradient Boosting	0.9464	0.9939	0.9464	0.9559	0.9454	0.9286	0.9321	0.3020
lightgbm	Light Gradient Boosting Machine	0.9429	0.9968	0.9429	0.9519	0.9419	0.9238	0.9272	1.0630
dt	Decision Tree Classifier	0.9283	0.9524	0.9283	0.9439	0.9274	0.9044	0.9099	0.1170
lr	Logistic Regression	0.9206	0.0000	0.9206	0.9315	0.9187	0.8942	0.8986	0.3410
lda	Linear Discriminant Analysis	0.8811	0.0000	0.8811	0.9103	0.8784	0.8416	0.8526	0.1100
qda	Quadratic Discriminant Analysis	0.8665	0.0000	0.8665	0.8978	0.8638	0.8219	0.8338	0.1080
nb	Naive Bayes	0.8624	0.9591	0.8624	0.8810	0.8557	0.8166	0.8255	0.1410
ada	Ada Boost Classifier	0.8593	0.0000	0.8593	0.8815	0.8579	0.8123	0.8203	0.2390
ridge	Ridge Classifier	0.8591	0.0000	0.8591	0.8732	0.8540	0.8122	0.8195	0.2160
knn	K Neighbors Classifier	0.8337	0.9520	0.8337	0.8700	0.8305	0.7783	0.7904	0.1750
svm	SVM - Linear Kernel	0.4437	0.0000	0.4437	0.4675	0.4106	0.2585	0.2828	0.1610
dummy	Dummy Classifier	0.2417	0.5000	0.2417	0.0586	0.0942	0.0000	0.0000	0.1560

- **F1 score:**

$$F1\ score = 2.\frac{Precision \times Recall}{Precision + Recall}$$

- **Cohen's Kappa:** is a statistical metric that measures the reliability of two raters rating the same thing, while taking into account the possibility that they could agree by chance. [3]
- **The Matthews correlation coefficient (MCC):** is a measure of the quality of binary (two-class) classifications, which ranges from -1 to +1. It's particularly useful when the classes are imbalanced.[4]
- **Training Time (TT):** The time spent to train a machine learning model, typically measured in seconds.

3.7 RESULTS :

3.7.1 Top Performance model :

Why CatBoost Stands Out:

High Accuracy & AUC : With an accuracy of 97.14% and an AUC near 1, the model demonstrates exceptional overall performance and discrimination power.
Excellent Recall : Ensures that almost all high-risk cases are detected , which is crucial in medical applications where missing a true positive can have serious consequences.
Strong Precision : Confirms that when the model predicts a patient is at risk, it is almost always correct — minimizing unnecessary alarms or interventions.
Balanced F1 Score : Reflects a well-rounded model that maintains both high precision and recall.
Robustness with Imbalanced Data : High Cohen's Kappa and MCC scores indicate reliable performance even after balancing the dataset using Random Over Sampler.
Training Time : While it takes 6.33 seconds to train — longer than simpler models like logistic regression — this is acceptable given its superior predictive power.

Medical Relevance:

In the context of radiotherapy planning , these results are particularly significant:

High-risk detection is perfect : Every high-risk case was identified, ensuring no critical patient is missed.

No false positives in "Safe" category : If the model labels a structure as safe, it truly is safe — a key requirement for clinical trust.

Only minor limitations in Safe class recall : A small number of safe cases were misclassified, but this does not compromise the model's core objective of identifying at-risk structures.

3.7.2 Important Features:

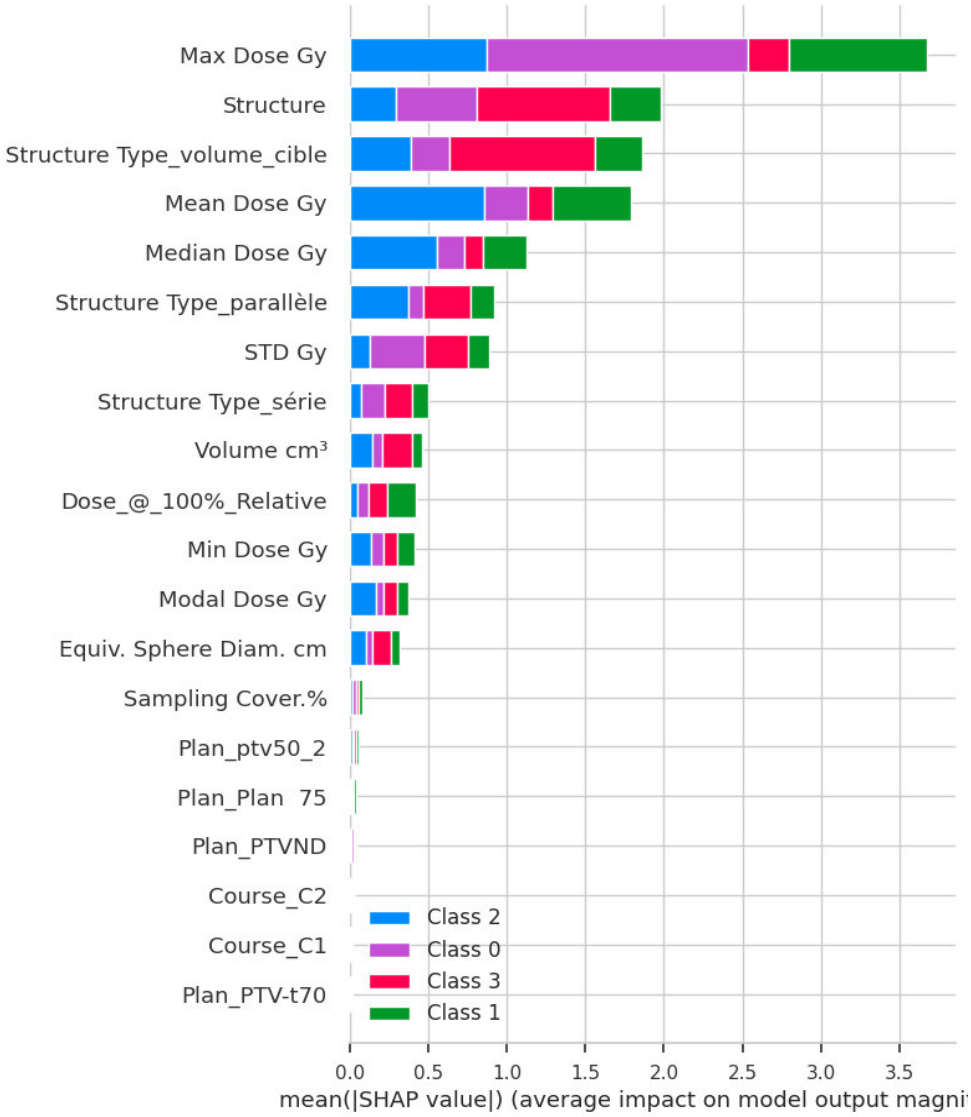

Figure 5 : Average impact on model output (Important Features).

In this model, the most influential features for determining patient risk categories are those related to radiation dose, specifically the maximum , mean , and median dose (all in Gy) . These dose metrics play a central role in assessing the likelihood of a structure being classified into a particular risk category.

The model appears to distinguish not only by how much radiation was delivered but also where it was delivered and the type of structure irradiated, since structural features such as Structure Name and Structure Type are quite influential.

For the High Risk and Medium Risk cases, the model places most of its emphasis on the maximum dose anatomic characteristics definition of the structure.

In contrast, Safe classifications are influenced by both the maximum dose and the average/central tendency of the dose (mean and median), indicating that lower and more evenly distributed doses are strongly associated with safer outcomes.

3.7.3 Classification Report:

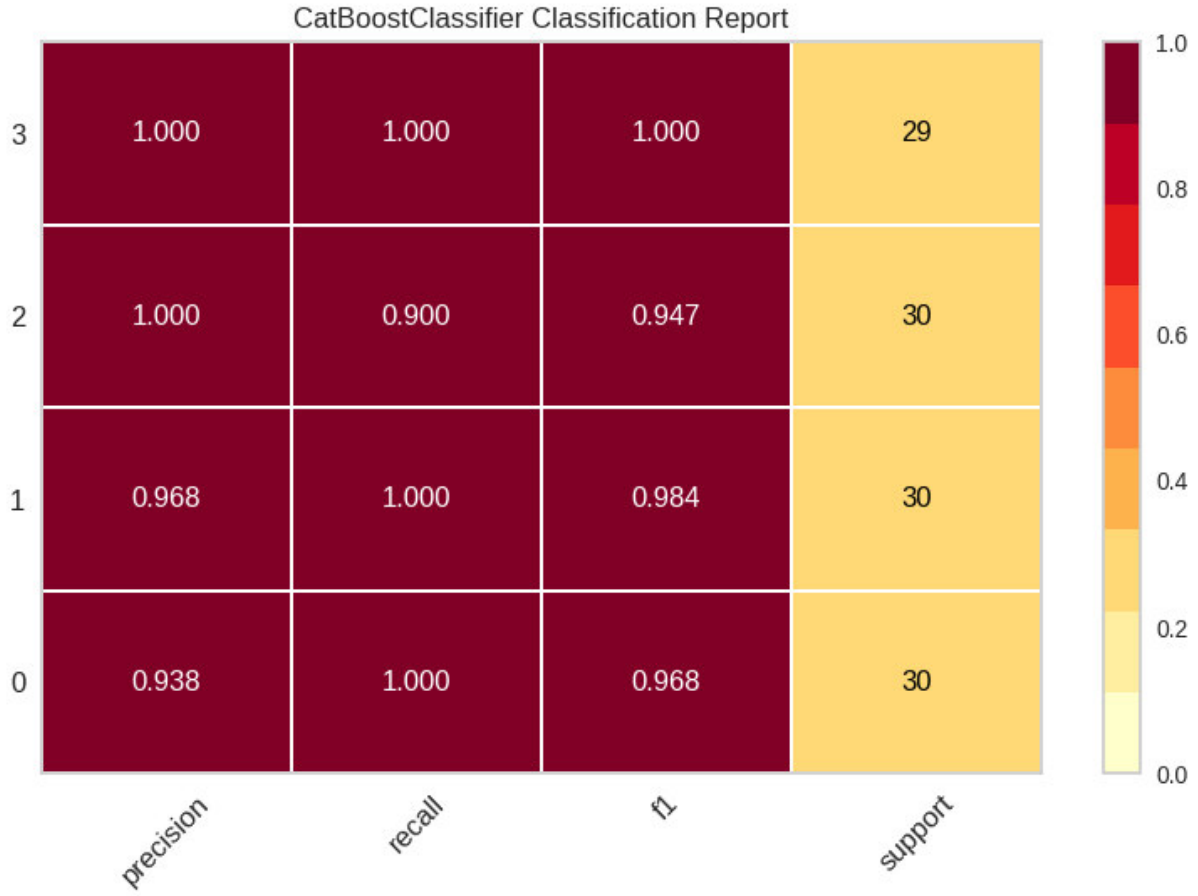

Figure6 : Catboost Classifier model Report.

Figure 6 represents a heatmap of precision, recall, f1 score and support of each class (safe, high risk, medium risk, unknown).

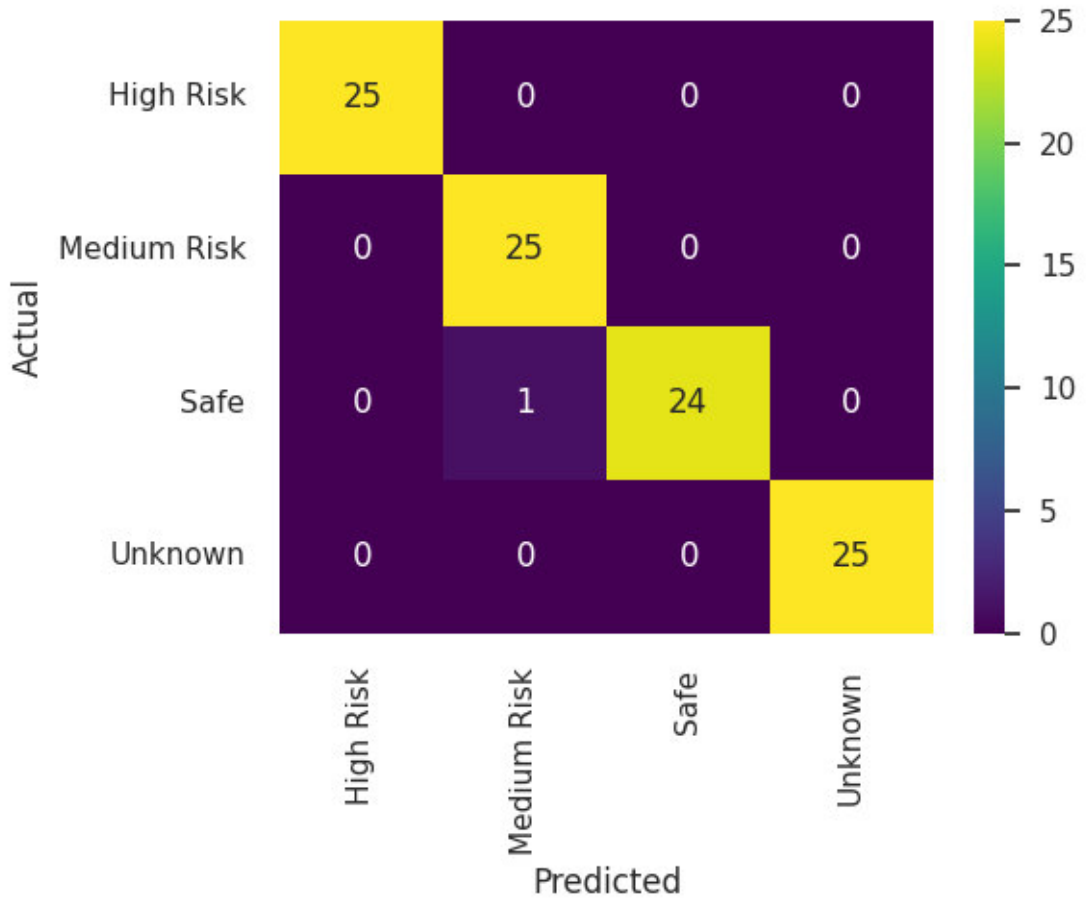

Figure 7: Confusion Matrix on Test Set

Figure 7 is a heatmap represents the confusion matrix of the test set. We can notice that: only one safe patient was not identified as such (1 patient out of 25).

Risk Class Performance Metrics

Characteristic	High Risk	Medium Risk	Safe	Unknown
Recall	100%	100%	90%	100%
Precision	93.8%	High	100%	100%
F1 Score	96.8%	98.4%	Good	Perfect

Table 05 : Risk class performance metrics

- **High risk (class 0):**
  - **Recall:** Every real high-risk instance was accurately recognized.
  - **precision:** 93.8% of predicted high-risk cases were indeed high-risk.
  - **F1 score:** Excellent performance all around **(**96.8%).
- **Medium risk (class 1):**
  - **Recall:** No incidents of medium risk were overlooked.
  - **precision:** False positives rarely occur.
  - **F1 score:** Excellent performance all around **(**98.4%).
- **Safe (class 2):**
  - **Recall:** 90% of safe cases were appropriately detected (10% were overlooked).
  - **Precision:** Every safe case that was anticipated was actually safe.
  - **F1 score:** Recall might be enhanced, but it is good.
- **Unknown (class 3):**
  - **Perfect scores:** Every unidentified case was accurately and solely found**.**

3.7.4 Summary:

3.7.4.1 Positives Points:

- The model's ability to detect all high and medium risk patients is incredibly good, which is critical in the medical field.
- Patients who are classified as safe are actually safe; there are no false positives for the safe category.

3.7.4.2 Negatives Points:

- The only minor flaw in recall for the safe class is that some safe patients were not identified as such (3 patients out of 30).

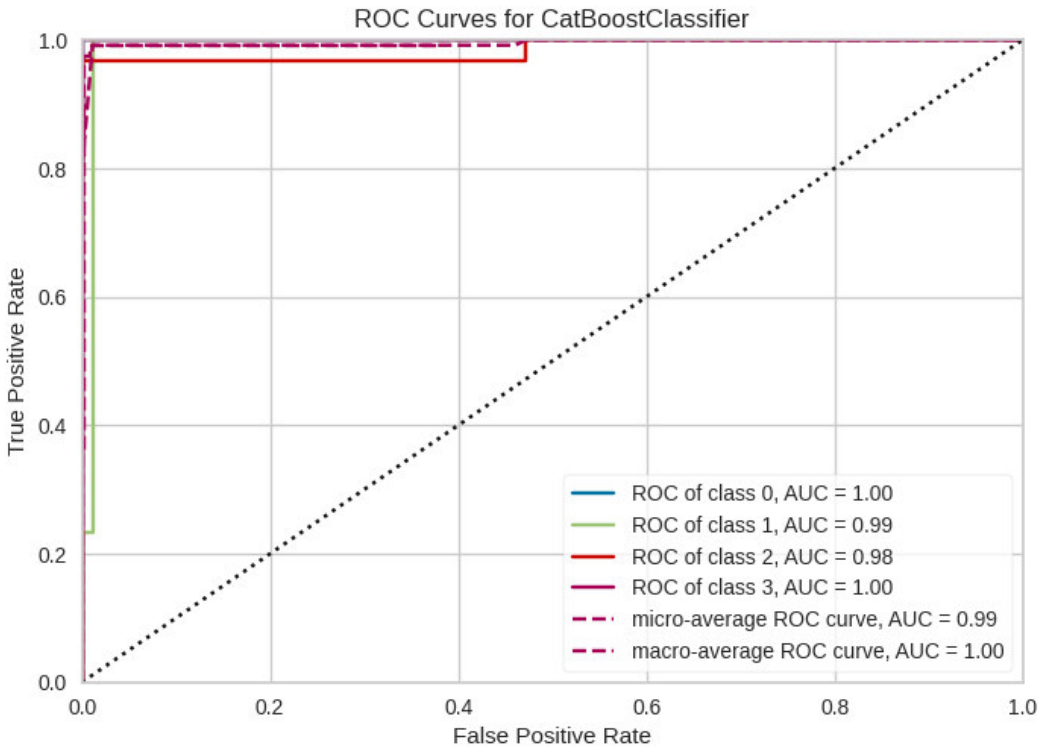

Figure 8: ROC curves for Catboost classifier.

3.8 Conclusion

This chapter presented a comprehensive workflow for building and evaluating a predictive classification model using the Pycaret library , aimed at assessing the risk categories of Organs at Risk (OARs) during radiotherapy treatment planning .

The dataset used in this study contained 228 anatomical structures from 10 patients, with each structure described by 19 features including dose metrics , anatomical structure types , and other clinical and categorical variables. The main objective was to classify each structure into one of four categories: Safe , Medium Risk , High Risk , or Unknown , to support better decision-making in radiation protection strategies.

Conclusion

4 General conclusion

In this thesis, Artificial intelligence was applied to model radiation beam behavior in radiotherapy, particularly to improve the classification of organs at risk (OARs) to ensure their protection. Starting with an introduction to radiotherapy history and the relevance of delivering doses accurately, the study demonstrates how recent advances in AI, especially machine learning, can be leveraged to improve beam modeling accuracy andreduce certain manual planning errors, thereby aiming to personalize treatment for each patient. Using real clinical data to develop an AI-driven decision model, the study developed algorithms that classify OARs into risk levels and generate predictive outputs to support medical decision-making. the results of this research demonstrate how AI-driven interventions can transform radiotherapy workflows and offer new perspectives for research and clinical implementation.

5 Limitations and Recommendations:

5.1 Limitations:

The challenge was the difficulty with obtaining clinical data due to privacy concerns and administrative procedures, which took a lot of time and effort to explain the safety and potential use of AI whilst keeping patient confidentiality intact. Additionally, the number of data was 10 patients so this is a very small dataset and the short time frame imposed further constraints on model, however the performance and validation were acceptable.

5.2 Recommendations:

To improve future research and clinical application of AI in radiotherapy, it would be helpful to create a shared and approved database to support research and benefit everyone involved. Also, adding more patient data will improve the AI model's ability to classify organs automatically during treatment planning. This may help to minimizing planning time and improve safety , also in future focusing on expande the dataset used to train the AI model, allowing it to classify organs during treatment planning more accurately. with hope to help reduce planning time and enhance decision-making for better patient safety. why not for the next research , we can add to this model functionalities such as automatic calculation of the Homogeneity Index (HI) and other dosimetric indicators that may support treatment evaluation and optimization.

References

References

Chapter One

Part 01 :

References :

1. *The Nobel Prize in Physics 1901 – Wilhelm Conrad Röntgen (Biographical)*. NobelPrize.org. Available at: https://www.nobelprize.org/prizes/physics/1901/rontgen/biographical/
2. S. Gianfaldoni *et al.*, "An overview on radiotherapy: From its history to its current applications in dermatology," *Open Access Maced. J. Med. Sci.*, vol. 5, no. 4, pp. 521–525, 2017. doi: 10.3889/oamjms.2017.122.
3. M. Tubiana, "Wilhelm Conrad Röntgen and the discovery of X-rays," *Bull. Acad. Natl. Med.*, vol. 180, no. 1, pp. 97–108, Jan. 1996. [Online]. Available: https://pubmed.ncbi.nlm.nih.gov/8696882/
4. F. Cmrečak, I. Andrašek, M. Solak Mekić, M. Ravlić, and L. Beketić-Orešković, "Modern radiotherapy techniques," *Libri Oncologici*, vol. 47, no. 2-3, Art. no. 17, 2019. doi: 10.20471/LO.2019.47.02-03.17.
5. K. Y. Cheung, "Intensity modulated radiotherapy: Advantages, limitations and future developments," *Biomed. Imaging Interv. J.*, vol. 2, no. 1, e19, 2006. doi: 10.2349/biij.2.1.e19.
6. C. Nutting, D. P. Dearnaley, and S. Webb, "Intensity modulated radiation therapy: A clinical review," *Br. J. Radiol.*, vol. 73, no. 869, pp. 459–469, 2000. doi: 10.1259/bjr.73.869.10884741.
7. Moffitt Cancer Center, "3D CRT (Three-Dimensional Conformal Radiation Therapy)," [Online]. Available: https://www.moffitt.org/treatments/radiation-therapy/3d-crt-three-dimensional-conformal-radiation-therapy/.
8. J. Lundkvist, M. Ekman, S. R. Ericsson, B. Jönsson, and B. Glimelius, "Proton therapy of cancer: Potential clinical advantages and cost-effectiveness," *Acta Oncol.*, vol. 44, no. 8, pp. 850–861, 2005, doi: 10.1080/02841860500341157.
9. Open Medscience, "Advancements in Proton Beam Therapy: A New Frontier in Cancer Treatment." [Online]. Available: https://openmedscience.com/advancements-in-proton-beam-therapy-a-new-frontier-in-cancer-treatment/.
10. A. R. Smith, "Proton therapy," *Phys. Med. Biol.*, vol. 51, no. 13, pp. R491–R504, Jun. 2006, doi: 10.1088/0031-9155/51/13/R26.
11. S. O. Hunte, C. H. Clark, N. Zyuzikov, and A. Nisbet, "Volumetric modulated arc therapy (VMAT): A review of clinical outcomes—what is the clinical evidence for the most effective implementation?," *Br. J. Radiol.*, vol. 94, no. 1117, p. 20201289, 2021. doi: 10.1259/bjr.20201289.
12. P. Knapp *et al.*, "The role of volumetric modulated arc therapy (VMAT) in gynaecological radiation therapy: A dosimetric comparison of intensity modulated

radiation therapy versus VMAT," *J. Med. Radiat. Sci.*, vol. 66, pp. 44–53, 2019. doi: 10.1002/jmrs.311.

13. [1] "Proton beam radiation therapy," *Dictionary of Cancer Terms*, National Cancer Institute. [Online]. Available: https://www.cancer.gov/publications/dictionaries/cancer-terms/def/proton-beam-radiation-therapy. [Accessed: Jun. 13, 2025].
14. [2] T. P. Howard, S. McClelland III, and R. B. Jimenez, "Evolving role of proton radiation therapy in clinical practice," *JCO Oncology Practice*, vol. 20, no. 6, Feb. 2024. [Online]. Available: https://doi.org/10.1200/OP.23.00674
15. H. M. Kooy and C. Grassberger, *Intensity modulated proton therapy*, Br. J. Radiol., vol. 88, no. 1051, p. 20150195, Jun. 17, 2015. [Online]. Available: https://doi.org/10.1259/bjr.20150195
16. H. Paganetti, P. Botas, G. C. Sharp, and B. Winey, *Adaptive proton therapy*, Phys. Med. Biol., vol. 66, no. 22, p. 10.1088/1361-6560/ac344f, Nov. 15, 2021. [Online]. Available: https://doi.org/10.1088/1361-6560/ac344f
17. K. Parodi, *Latest developments in in-vivo imaging for proton therapy*, Br. J. Radiol., vol. 93, no. 1107, p. 20190787, Feb. 14, 2020. [Online]. Available: https://doi.org/10.1259/bjr.20190787
18. C. Cunningham, M. de Kock, M. Engelbrecht, X. Miles, J. Slabbert, and C. Vandevoorde, *Radiosensitization effect of gold nanoparticles in proton therapy*, Front. Public Health, vol. 9, Jul. 29, 2021. [Online]. Available: https://doi.org/10.3389/fpubh.2021.699822
19. J. Ma, H. Shen, and Z. Mi, *Enhancing proton therapy efficacy through nanoparticle-mediated radiosensitization*, Cells, vol. 13, no. 22, p. 1841, Nov. 7, 2024. [Online]. Available: https://doi.org/10.3390/cells13221841
20. R. H. Press and M. P. Mehta, *Proton therapy: current status and controversies*, JCO Oncology Practice, vol. 20, no. 6, Mar. 28, 2024. [Online]. Available: https://doi.org/10.1200/OP.24.00132

Part 02 :

References :

1. AAPM Task Group 157, "Beam modeling and beam model commissioning for Monte Carlo dose calculation-based radiation therapy treatment planning: Report of AAPM Task Group 157," *Medical Physics*, 2019. Available: https://doi.org/10.1002/mp.13898.
2. J. B. Hansen and S. P. Frigo, "Evaluation of candidate template beam models for a matched TrueBeam treatment delivery system," *Journal of Applied Clinical Medical Physics*, 2023. Available: https://doi.org/10.1002/acm2.13278.
3. M. D. C. Evans, *Computerized Treatment Planning Systems for External Photon Beam Radiotherapy*, McGill University Health Centre, Montréal, Canada. Available: https://www.irsn.fr/sites/default/files/documents/professionnels_sante/documentation/syllabus_chapitre_11.pdf.

4. J. Chen *et al.*, "Optimizing Beam Models for Dosimetric Accuracy Over a Wide Range of Treatments," *Physica Medica: European Journal of Medical Physics*, vol. 60, pp. 1-11, 2019. doi: 10.1016/j.ejmp.2019.01.011.
5. Radiation protection," *Radiology Cafe*, Available: https://www.radiologycafe.com/frcr-physics-notes/radiation-dosimetry-protection-and-legislation/radiation-protection/.
6. What is the difference between Radioactivity, Radiation, and Radioactive Materials?" *Matsusada Precision*, Available: https://www.matsusada.com/column/whats_radiation.html.
7. P. P. Urone, R. Hinrichs, F. Gozuacik, D. Pattison, and C. Tabor, *Physics*, OpenStax, 2022. Available: https://assets.openstax.org/oscms-prodcms/media/documents/Physics-WEB_Sab7RrQ.pdf
8. "X-rays," *Science Topics*, National Institute of Biomedical Imaging and Bioengineering (NIBIB). [Online]. Available: https://www.nibib.nih.gov/science-education/science-topics/x-rays. [Accessed: Jun. 14, 2025]
9. Depth of penetration of radiation energy," *Nondestructive Evaluation Techniques: Radiography*, NDE-Ed.org. [Online]. Available: https://www.nde-ed.org/NDETechniques/Radiography/penetrationdepth.xhtml. [Accessed: Jun. 14, 2025]

Part 3 :

References :

1. H. Seo, C. Huang, M. Bassenne, *et al.*, "Modified U-Net (mU-Net) with incorporation of object-dependent high level features for improved liver and liver-tumor segmentation in CT images," *IEEE Trans. Med. Imaging*, vol. 39, no. 5, pp. 1316–1325, 2020, doi: 10.1109/TMI.2019.2948320.
2. B. Ibragimov and L. Xing, "Segmentation of organs-at-risk in head and neck CT images using convolutional neural networks," *Med. Phys.*, vol. 44, no. 2, pp. 547–557, 2017, doi: 10.1002/mp.12045.
3. F. Maes, A. Collignon, D. Vandermeulen, *et al.*, "Multimodality image registration by maximization of mutual information," *IEEE Trans. Med. Imaging*, vol. 16, no. 2, pp. 187–198, 1997, doi: 10.1109/42.563664.
4. G. E. Christensen, J. H. Song, W. Lu, *et al.*, "Tracking lung tissue motion and expansion/compression with inverse consistent image registration and spirometry," *Med. Phys.*, vol. 34, no. 6, pp. 2155–2163, 2007, doi: 10.1118/1.2731029.
5. V. K. Reed, W. A. Woodward, L. Zhang, *et al.*, "Automatic segmentation of whole breast using atlas approach and deformable image registration," *Int. J. Radiat. Oncol. Biol. Phys.*, vol. 73, no. 5, pp. 1493–1500, 2009, doi: 10.1016/j.ijrobp.2008.07.001.
6. L. A. Olteanu, I. Madani, W. De Neve, *et al.*, "Evaluation of deformable image coregistration in adaptive dose painting by numbers for head-and-neck cancer," *Int. J. Radiat. Oncol. Biol. Phys.*, vol. 83, no. 2, pp. 696–703, 2012, doi: 10.1016/j.ijrobp.2011.07.037.

7. G. Balakrishnan, A. Zhao, M. R. Sabuncu, *et al*., "VoxelMorph: A learning framework for deformable medical image registration," *IEEE Trans. Med. Imaging*, 2019, doi: 10.1109/TMI.2019.2897538.
8. H. Xiao, X. Teng, C. Liu, *et al*., "A review of deep learning-based three-dimensional medical image registration methods," *Quant. Imaging Med. Surg.*, vol. 11, no. 12, pp. 4895–4916, 2021, doi: 10.21037/qims-21-175.
9. X. Teng, Y. Chen, Y. Zhang, *et al*., "Respiratory deformation registration in 4DCT/cone beam CT using deep learning," *Quant. Imaging Med. Surg.*, vol. 11, no. 2, pp. 737–748, 2021, doi: 10.21037/qims-19-1058.
10. B. Zhu, J. Z. Liu, S. F. Cauley, *et al*., "Image reconstruction by domain-transform manifold learning," *Nature*, vol. 555, no. 7697, pp. 487–492, 2018, doi: 10.1038/nature25988.
11. J. Liu, H. Xiao, J. Fan, W. Hu, Y. Yang, P. Dong, L. Xing, and J. Cai, "An overview of artificial intelligence in medical physics and radiation oncology," *J. Natl. Cancer Cent.*, 2023, doi: 10.1016/j.jncc.2023.08.002.
12. L. Shen, W. Zhao, and L. Xing, "Patient-specific reconstruction of volumetric computed tomography images from a single projection view via deep learning," *Nat. Biomed. Eng.*, vol. 3, no. 11, pp. 880–888, 2019, doi: 10.1038/s41551-019-0466-4.
13. Y. LeCun, Y. Bengio, and G. Hinton, "Deep learning," *Nature*, vol. 521, no. 7553, pp. 436–444, 2015, doi: 10.1038/nature14539.
14. W. Zhao, B. Han, Y. Yang, *et al*., "Incorporating imaging information from deep neural network layers into image guided radiation therapy (IGRT)," *Radiother. Oncol.*, vol. 140, pp. 167–174, 2019, doi: 10.1016/j.radonc.2019.06.027.
15. W. Zhao, L. Shen, B. Han, *et al*., "Markerless pancreatic tumor target localization enabled by deep learning," *Int. J. Radiat. Oncol. Biol. Phys.*, vol. 105, no. 2, pp. 432–439, 2019, doi: 10.1016/j.ijrobp.2019.05.071.
16. W. Zhao, B. Han, Y. Yang, *et al*., "Visualizing the invisible in prostate radiation therapy: markerless prostate target localization via a deep learning model and monoscopic kV projection X-ray image," *Int. J. Radiat. Oncol. Biol. Phys.*, vol. 102, no. 3, suppl. 1, pp. S128–S129, 2018, doi: 10.1016/j.ijrobp.2018.06.319.
17. J. Fan, L. Xing, P. Dong, *et al*., "Data-driven dose calculation algorithm based on deep U-Net," *Phys. Med. Biol.*, vol. 65, no. 24, p. 245035, 2020, doi: 10.1088/1361-6560/abca05.
18. G. Valdes, R. Scheuermann, C. Y. Hung, *et al*., "A mathematical framework for virtual IMRT QA using machine learning," *Med. Phys.*, vol. 43, no. 7, p. 4323, 2016, doi: 10.1118/1.4953835.
19. J. Fan, L. Xing, and Y. Yang, "Independent verification of brachytherapy treatment plan by using deep learning inference modeling," *Phys. Med. Biol.*, vol. 66, no. 12, 2021, doi: 10.1088/1361-6560/ac067f.
20. M. Yue, X. Xue, Z. Wang, *et al*., "Dose prediction via distance-guided deep learning: Initial development for nasopharyngeal carcinoma radiotherapy," *Radiother. Oncol.*, vol. 170, pp. 198–204, 2022, doi: 10.1016/j.radonc.2022.03.012.

21. B. Ibragimov, D. A. Toesca, Y. Yuan, *et al*., "Deep 3D dose analysis for prediction of outcomes after liver stereotactic body radiation therapy," in *Medical Image Computing and Computer Assisted Intervention – MICCAI 2018*, A. Frangi, J. Schnabel, C. Davatzikos, C. Alberola-López, and G. Fichtinger, Eds., Lecture Notes in Computer Science, vol. 11071. Springer, 2018, pp. 684–692, doi: 10.1007/978-3-030-00934-2_76.
22. B. Ibragimov, D. A. S. Toesca, D. T. Chang, *et al*., "Deep learning for identification of critical regions associated with toxicities after liver stereotactic body radiation therapy," *Med. Phys.*, vol. 47, no. 8, pp. 3721–3731, 2020, doi: 10.1002/mp.14235.
23. J. E. Bibault, D. T. Chang, and L. Xing, "Development and validation of a model to predict survival in colorectal cancer using a gradient-boosted machine," *Gut*, vol. 70, no. 5, pp. 884–889, 2021, doi: 10.1136/gutjnl-2020-321799.
24. J. Liu, L. Yang, J. L. Zhang, *et al*., "Integrate sequence information of dose volume histogram in training LSTM-based deep learning model for lymphopenia diagnosis," *Int. J. Radiat. Oncol. Biol. Phys.*, vol. 111, no. 3, pp. e112–e113, 2021, doi: 10.1016/j.ijrobp.2021.07.520.
25. A. L. Appelt, B. Elhaminia, A. Gooya, *et al*., "Deep learning for radiotherapy outcome prediction using dose data – a review," *Clin. Oncol. (R. Coll. Radiol.)*, vol. 34, no. 2, pp. e87–e96, 2022, doi: 10.1016/j.clon.2021.12.002

AI chapter :
References :

[1] J. Brownlee, "Classification and Regression Trees for Machine Learning," *Machine Learning Mastery*, [Online]. Available: https://machinelearningmastery.com/classification-and-regression-trees-for-machine-learning/

[2] Université de Médéa, "Cours sur les arbres de décision (CTI)," [Online]. Available: http://moodle.univ-medea.dz/pluginfile.php/20012/mod_resource/content/1/CTI.pdf

[3] Techno-Science.net, "Machine à vecteurs de support - Page 2," [Online]. Available: https://www.techno-science.net/glossaire-definition/Machine-a-vecteurs-de-support-page-2.html

[4] A. V., "Regression Analysis in Machine Learning," *Avatpoint*, [Online]. Available: avatpoint.com/regression-analysis-in-machine-learning

[5] M. Geist, "Paradigme général de l'apprentissage par renforcement," *ResearchGate*, [Online]. Available: https://www.researchgate.net/profile/Matthieu-Geist/publication/40660047/figure/fig1/AS:669460713197570@1536623280207

[6] Juripredis, "Réseaux de neurones feed-forwarded," [Online]. Available: https://www.juripredis.com/upload/actualites/Machine_learning/reseaux_neurones_feed_forwarded.png

References

[7] V. Sokeng, “Un réseau multicouche,” *ResearchGate*, [Online]. Available: https://www.researchgate.net/profile/Valere-Sokeng-2/publication/304570524/figure/fig1/AS:378243929657344@1467191788485

[8] Echoradar, “Inceptionisme : le neuron-art selon Google,” [Online]. Available: https://echoradar.eu/2015/07/04/inceptionisme-le-neuron-art-selon-google/

[9] Echoradar, “Inceptionisme : le neuron-art selon Google,” [Online]. Available: https://echoradar.eu/2015/07/04/inceptionisme-le-neuron-art-selon-google/

[10] J. Brownlee, “How to Choose an Activation Function for Deep Learning,” *Machine Learning Mastery*, [Online]. Available: https://machinelearningmastery.com/choose-an-activation-function-for-deep-learning/

[11] DataScience.eu, “Comprendre les réseaux de neurones,” [Online]. Available: https://datascience.eu/fr/apprentissage-automatique/comprendre-les-reseaux-de-neurones/

[12] Data Analytics Post, “Réseaux de neurones récurrents,” [Online]. Available: https://dataanalyticspost.com/Lexique/reseaux-de-neurones-recurrents/

[13] Wikipédia, “Machine de Boltzmann restreinte,” [Online]. Available: https://fr.wikipedia.org/wiki/Machine_de_Boltzmann_restreinte

[14] Wikipedia, “Boltzmann machine,” [Online]. Available: https://en.wikipedia.org/wiki/Boltzmann_machine

[15] My Little Neuron, “Machine Learning: La machine de Boltzmann restreinte,” [Online]. Available: https://mylittleneuron.com/2020/10/20/machine-learning-la-machine-de-boltzmann-restreinte .

Chapter Two :

References :

1. C. M. Ma *et al.*, "Beam modeling and beam model commissioning for Monte Carlo dose calculation-based radiation therapy treatment planning: Report of AAPM Task Group 157," *Med. Phys.*, vol. 47, no. 4, pp. e101–e119, 2020, doi: 10.1002/mp.14064.
2. J. Chen *et al.*, "Optimizing beam models for dosimetric accuracy over a wide range of treatments," *Phys. Med. Eur. J. Med. Phys.*, vol. 61, pp. 36–42, 2019, doi: 10.1016/j.ejmp.2019.01.011.
3. M. Kawamura *et al.*, "Revolutionizing radiation therapy: the role of AI in clinical practice," *J. Radiat. Res.*, vol. 65, no. 1, pp. 1–9, 2024, doi: 10.1093/jrr/rrad090.
4. G. Landry, C. Kurz, and A. Traverso, "The role of artificial intelligence in radiotherapy clinical practice," *Br. J. Radiol. Open*, vol. 5, 2023, Art. no. 20230030, doi: 10.1259/bjro.20230030.

References

Chapter four :

References:

[1]: https://pycaret.gitbook.io/docs

[2]: https://www.analyticsvidhya.com/blog/2021/07/metrics-to-evaluate-your-classification-model-to-take-the-right-decisions/#h-what-is-confusion-matrix

[3]: https://builtin.com/data-science/cohens-kappa

[4]: https://medium.com/@anishnama20/matthews-correlation-coefficient-mcc-one-of-the-best-metric-when-2-classes-are-imbalanced-c0318ac68c21

ANNEX (prediction code)

Thanks

At the end of this long and enriching journey, I would like to express my deepest gratitude to everyone who supported me throughout the completion of this thesis.

First and foremost, I extend my heartfelt thanks to my supervisor, Dr. Boufateh Mohammed Reda , and my co-supervisor, Bensaber Fatima Zahra , for their invaluable guidance, continuous support, and constructive feedback. Their expertise and encouragement were instrumental in shaping this work and helping me overcome various challenges along the way.

I am sincerely grateful to the members of the thesis jury for generously dedicating their time and effort to review and evaluate this research. Their insightful comments and suggestions have significantly contributed to improving the quality of this thesis.

I would also like to thank all the professors and colleagues at the university for their academic support, stimulating discussions, and kind words throughout my studies. Their contributions have greatly enriched my learning experience and deepened my understanding of the subject matter.

I am deeply thankful to my family—my parents, my siblings, and my extended family—for their unwavering love, prayers, and encouragement. Their constant support has been the foundation of my success and motivation throughout this journey.

To my dear friends and loved ones: your kindness, patience, and moral support during challenging times have made this endeavor possible. Your presence brought joy and strength when it was needed most.

Finally, I would like to thank Dahi EL-hadj chef medical physicist at the Anti-Cancer Center – Tlemcen , for providing the clinical data used in this study. Their efforts in collecting and maintaining patient records made this research feasible and relevant.

This work is dedicated to all those who believed in me, inspired me, and walked with me—directly or indirectly—on this academic path.

Thank you.

```
pip install pycaret[analysis,models]
```

Afficher la sortie masquée

Import Required Libraries

```
import numpy as np
import pandas as pd
import pycaret
import seaborn as sns
import matplotlib.pyplot as plt
from pycaret.classification import *
```

Load and Inspect the Dataset

```
df=pd.read_csv('/content/PATIENTS.csv',delimiter=',')
df.head()
```

	Unnamed: 0	Structure	Approval Status	Plan	Course	Volume [cm³]	Dose Cover. [%]	Sampling Cover. [%]	Min Dose [Gy]	Max Dose [Gy]	...	D_76	D_81	D_86	D_91	D_96	
0	0	body	Approuvée	ptv50_2	C2	15243.4	100.0	100.0	0.000	75.079	...	0.752674	0.645113	0.537627	0.412107	0.225251	0.08
1	1	BrainStem	Approuvée	ptv50_2	C2	68.0	100.0	100.0	1.974	45.551	...	3.943869	3.346838	2.925238	2.611056	2.354322	2.16
2	2	Eye_L	Approuvée	ptv50_2	C2	12.5	100.0	100.1	1.090	4.598	...	2.129410	2.056807	1.978929	1.891812	1.778599	1.66
3	3	Eye_R	Approuvée	ptv50_2	C2	12.4	100.0	100.0	0.932	4.549	...	2.206683	2.130403	2.049012	1.958258	1.844407	1.73
4	4	LARYNX	Approuvée	ptv50_2	C2	46.4	100.0	100.0	18.613	63.543	...	24.948599	24.208884	23.473555	22.717565	21.824018	20.7

5 rows × 42 columns

Preprocess / Clean the Data

```
df.columns
```

```
Index(['Unnamed: 0', 'Structure', 'Approval Status', 'Plan', 'Course',
       'Volume [cm³]', 'Dose Cover.[%]', 'Sampling Cover.[%]', 'Min Dose [Gy]',
       'Max Dose [Gy]', 'Mean Dose [Gy]', 'Modal Dose [Gy]',
       'Median Dose [Gy]', 'STD [Gy]', 'Equiv. Sphere Diam. [cm]',
       'Conformity Index', 'Gradient Measure [cm]', 'D_1', 'D_6', 'D_11',
       'D_16', 'D_21', 'D_26', 'D_31', 'D_36', 'D_41', 'D_46', 'D_51', 'D_56',
       'D_61', 'D_66', 'D_71', 'D_76', 'D_81', 'D_86', 'D_91', 'D_96', 'D_99',
       'Dose_@_100%_Relative', 'Structure Type', 'homoginity_index',
       'OAR Evaluation'],
      dtype='object')
```

```
df.drop(columns=['Unnamed: 0','homoginity_index','D_1', 'D_6', 'D_11',
       'D_16', 'D_21', 'D_26', 'D_31', 'D_36', 'D_41', 'D_46', 'D_51', 'D_56',
       'D_61', 'D_66', 'D_71', 'D_76', 'D_81', 'D_86', 'D_91', 'D_96', 'D_99'],inplace=True)
```

```
df.columns
```

```
Index(['Structure', 'Approval Status', 'Plan', 'Course', 'Volume [cm³]',
       'Dose Cover.[%]', 'Sampling Cover.[%]', 'Min Dose [Gy]',
       'Max Dose [Gy]', 'Mean Dose [Gy]', 'Modal Dose [Gy]',
       'Median Dose [Gy]', 'STD [Gy]', 'Equiv. Sphere Diam. [cm]',
       'Conformity Index', 'Gradient Measure [cm]', 'Dose_@_100%_Relative',
       'Structure Type', 'OAR Evaluation'],
      dtype='object')
```

```
import matplotlib.pyplot as plt
import seaborn as sns

plt.figure(figsize=(8, 5))
sns.histplot(df['OAR Evaluation'], bins=30, kde=True, color='skyblue')
plt.title("Distribution of OAR Evaluation")
plt.xlabel("OAR Evaluation")
plt.ylabel("Number of Structures")
plt.tight_layout()
plt.show()
```

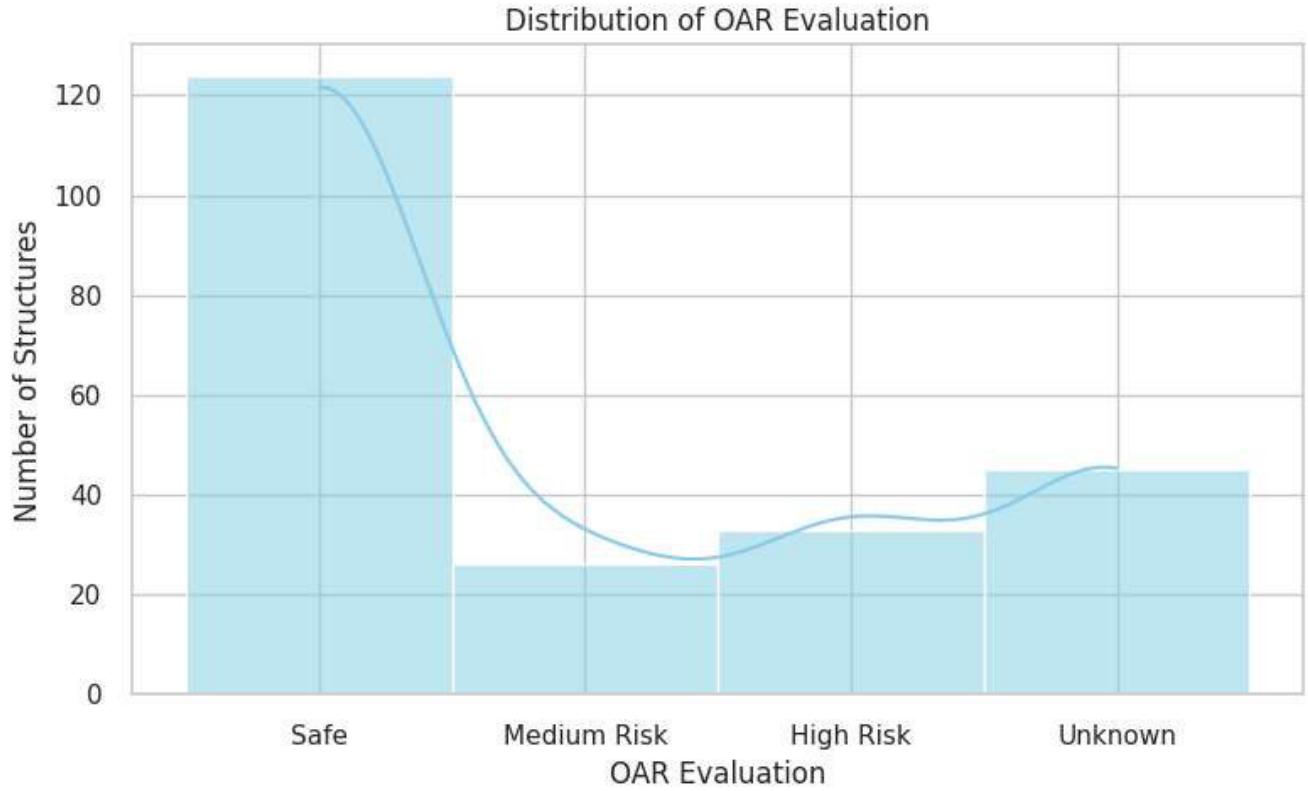


```
np.random.seed(42)
df['Mean Dose [Gy]'] = np.random.normal(loc=50, scale=10, size=len(df))

plt.figure(figsize=(9, 5))
sns.boxplot(data=df, x='OAR Evaluation', y='Mean Dose [Gy]', hue='Structure Type', palette='Set2')
plt.title("Mean Dose Distribution by OAR Evaluation and Structure Type", fontweight='bold')
plt.xlabel("OAR Evaluation", fontweight='bold')
plt.ylabel("Mean Dose [Gy]", fontweight='bold')
plt.legend(title='Structure Type')
plt.tight_layout()
plt.show()
```

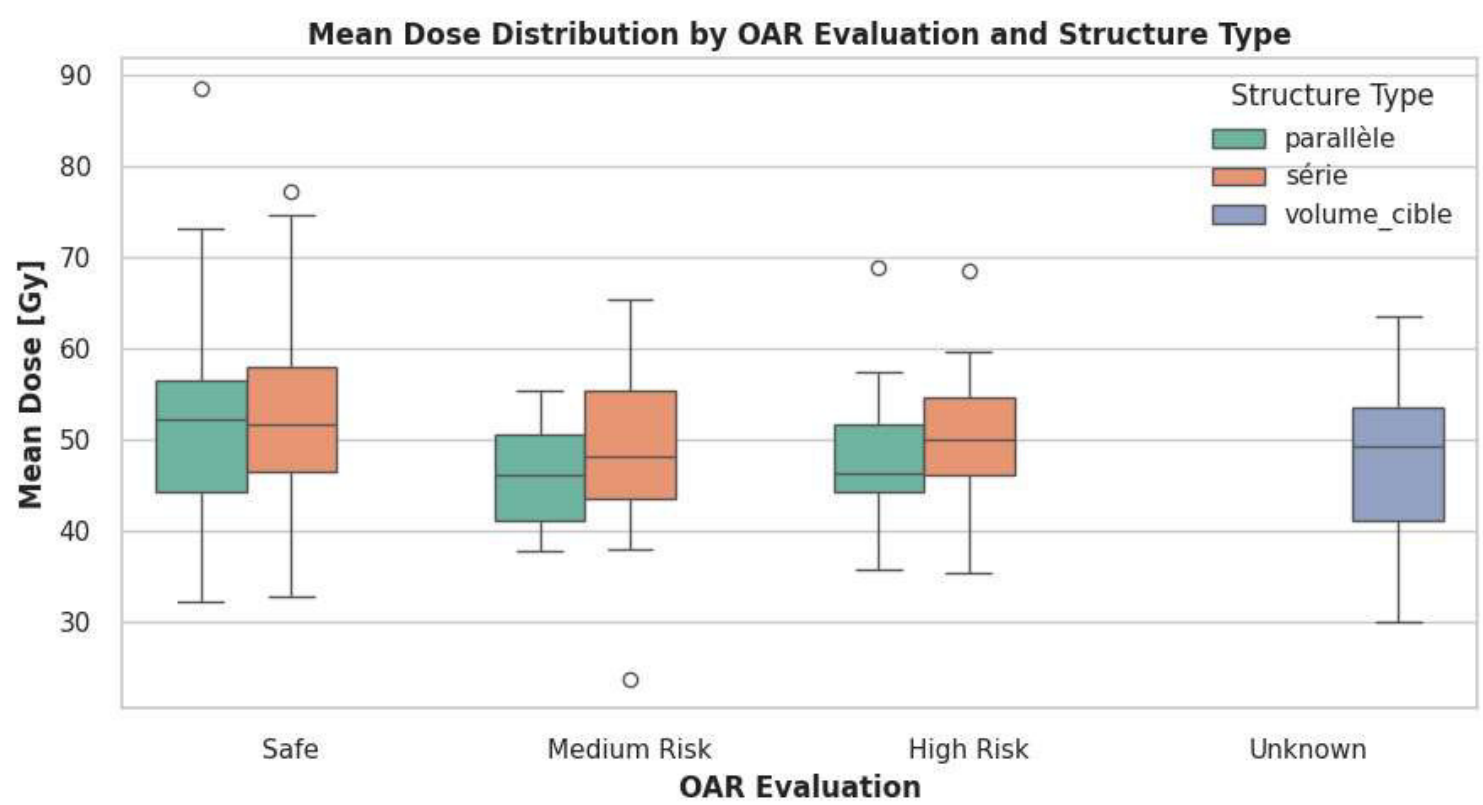


```
df['Structure'].unique()
```

```
array(['body', 'BrainStem', 'Eye_L', 'Eye_R', 'LARYNX', 'Lens_L',
       'Lens_R', 'OpticNerve_L', 'OpticNerve_R', 'Oral Cavity',
       'Parotid_L', 'Parotid_R', 'ptv-T70', 'PTV56', 'Spinal Cord',
       'TemporalLobe_L', 'TemporalLobe_R', 'Thyroid1', 'PTVp70',
       'PRV_spinal', 'PRV_brainstem', 'spinal cord', 'PTVN-L1', 'PTVN-L2',
       'PTVN-D', 'PTV t 70', 'PTVTN', 'PTV t 63', 'Pituitary', 'PTV 70',
       'PTV 63', 'Mandible', 'PTV50', 'Chiasm', 'Brain', 'OREILLE INT GH',
       'OREILLE INT DT', 'PTV-60', 'PTV-66', 'Thyroid', 'CTVTN', 'CTVp',
       'GTVP', 'PTVN-boost-LEFT', 'Larynx', 'parotid-right',
       'parotid-left', 'PTVN-boost-RIGHT', 'PTVPBOOST', 'GTVnDT', 'CTVt',
       'PTV01', 'PTV02', 'PTV03dt', 'PTV04ghe', 'brain', 'GTVp'],
      dtype=object)
```

```
# Visualizations using the 'Structure' feature and 'OAR Evaluation'
```

```
# Set plot style
import seaborn as sns
import matplotlib.pyplot as plt

sns.set(style="whitegrid")
custom_palette = {
    'High Risk': 'red',
    'Medium Risk': 'orange',
    'Unknown': 'gray',
    'Safe': 'green'
}

# 1. Countplot: Distribution of OAR Evaluation per Structure
plt.figure(figsize=(12, 6))
sns.countplot(data=df, x='Structure', hue='OAR Evaluation', palette=custom_palette)
plt.title("OAR Evaluation Distribution per Structure", fontweight='bold')
plt.xlabel("Structure", fontweight='bold')
plt.ylabel("Count", fontweight='bold')
plt.legend(title='OAR Evaluation', bbox_to_anchor=(1, 1),loc='best')
plt.xticks(rotation=45)
plt.tight_layout()
plt.show()
```

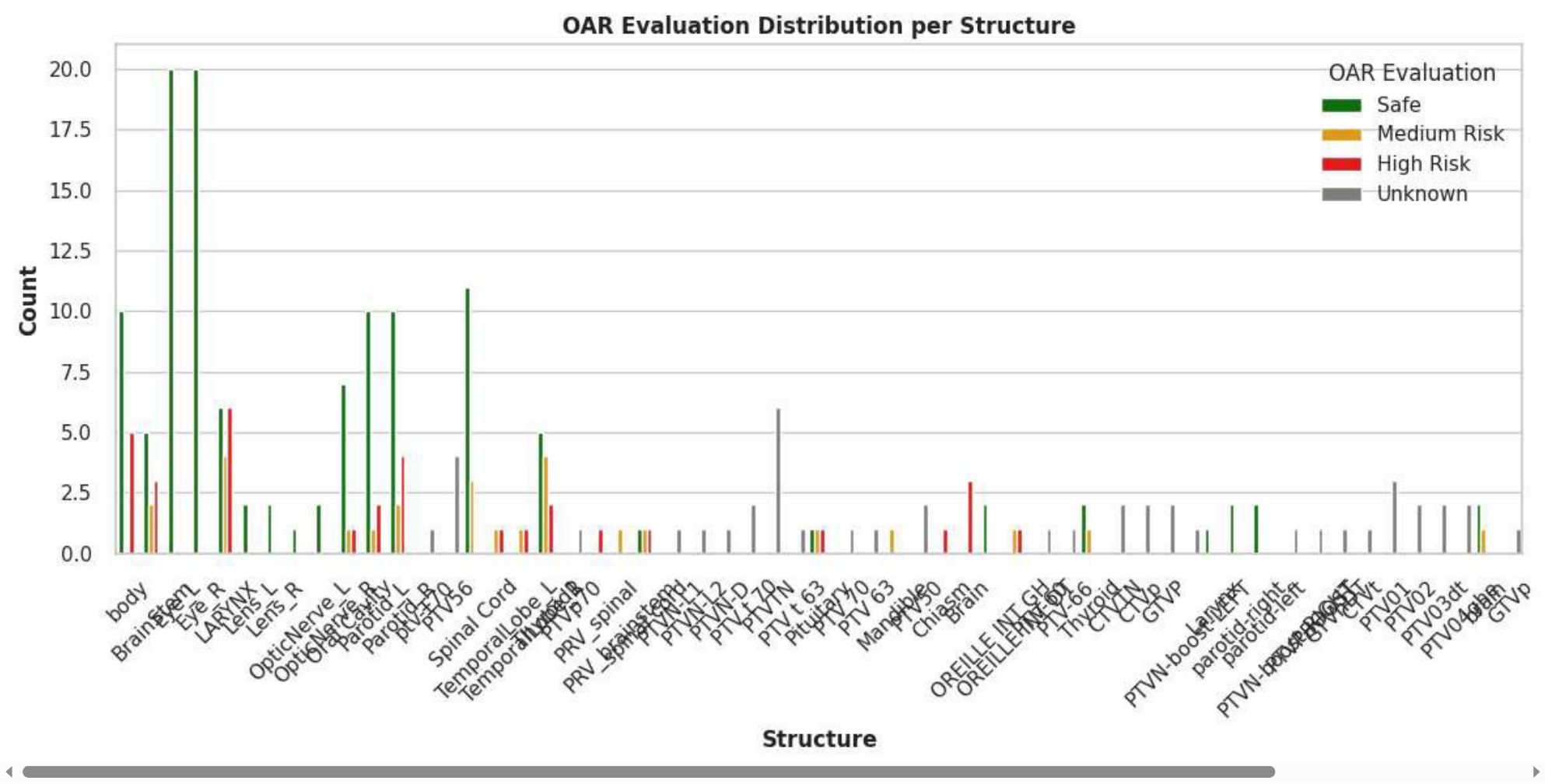


```
# Drop rows with missing target
data_class = df.dropna(subset=['OAR Evaluation'])


# the distribution of classes
data_class['OAR Evaluation'].value_counts(normalize=True)
```

OAR Evaluation	proportion
Safe	0.543860
Unknown	0.197368
High Risk	0.144737
Medium Risk	0.114035

dtype: float64

```
structure_map = {
    # SpinalCord variants
    'Spinal Cord': 'SpinalCord',
    'spinal cord': 'SpinalCord',
    'PRV spinal': 'SpinalCord',

    # Parotid_L variants
    'Parotid_L': 'Parotid_L',

    # Parotid_R variants
    'Parotid_R': 'Parotid_R',
    'parotid-right': 'Parotid_R',

    # BrainStem variants
    'BrainStem': 'BrainStem',
    'Brain': 'BrainStem',
    'brain': 'BrainStem',

    # Eye_L and Eye_R
    'Eye_L': 'Eye_L',
    'Eye_R': 'Eye_R',

    # PTV56 and similar
    'PTV56': 'PTV56',
    'PTV 56': 'PTV56',
    'PTV-L1': 'PTV56',
    'PTV 70': 'PTV56',
    'PTVp70': 'PTV56',
    'PTVPBOOST': 'PTV56',
    'PTVN-boost-LEFT': 'PTV56',
    'PTV04ghe': 'PTV56',
```

```
        'PTV02': 'PTV56',
        'PTV-66': 'PTV56',
        'PTV t 70': 'PTV56',
        'PTVN-L1': 'PTV56',
    }
    data_class['Structure'] = data_class['Structure'].replace(structure_map)
    selected_structures = ['PTV56', 'SpinalCord', 'Parotid_L', 'Eye_R', 'Eye_L', 'Parotid_R', 'BrainStem']
    filtered_data = data_class[data_class['Structure'].isin(selected_structures)]

    pivot_table = filtered_data.pivot_table(
        values='Mean Dose [Gy]',
        index='Structure',
        columns='OAR Evaluation',
        aggfunc='mean'
    )

    plt.figure(figsize=(12, 6))
    sns.heatmap(pivot_table, annot=True, fmt=".1f", cmap='RdYlGn', linewidths=0.5, cbar_kws={'label': 'Mean Dose [Gy]'})
    plt.title("Mean Dose [Gy] by Structure and OAR Evaluation", fontweight='bold')
    plt.xlabel("OAR Evaluation", fontweight='bold')
    plt.ylabel("Structure", fontweight='bold')
    plt.tight_layout()
    plt.show()
```

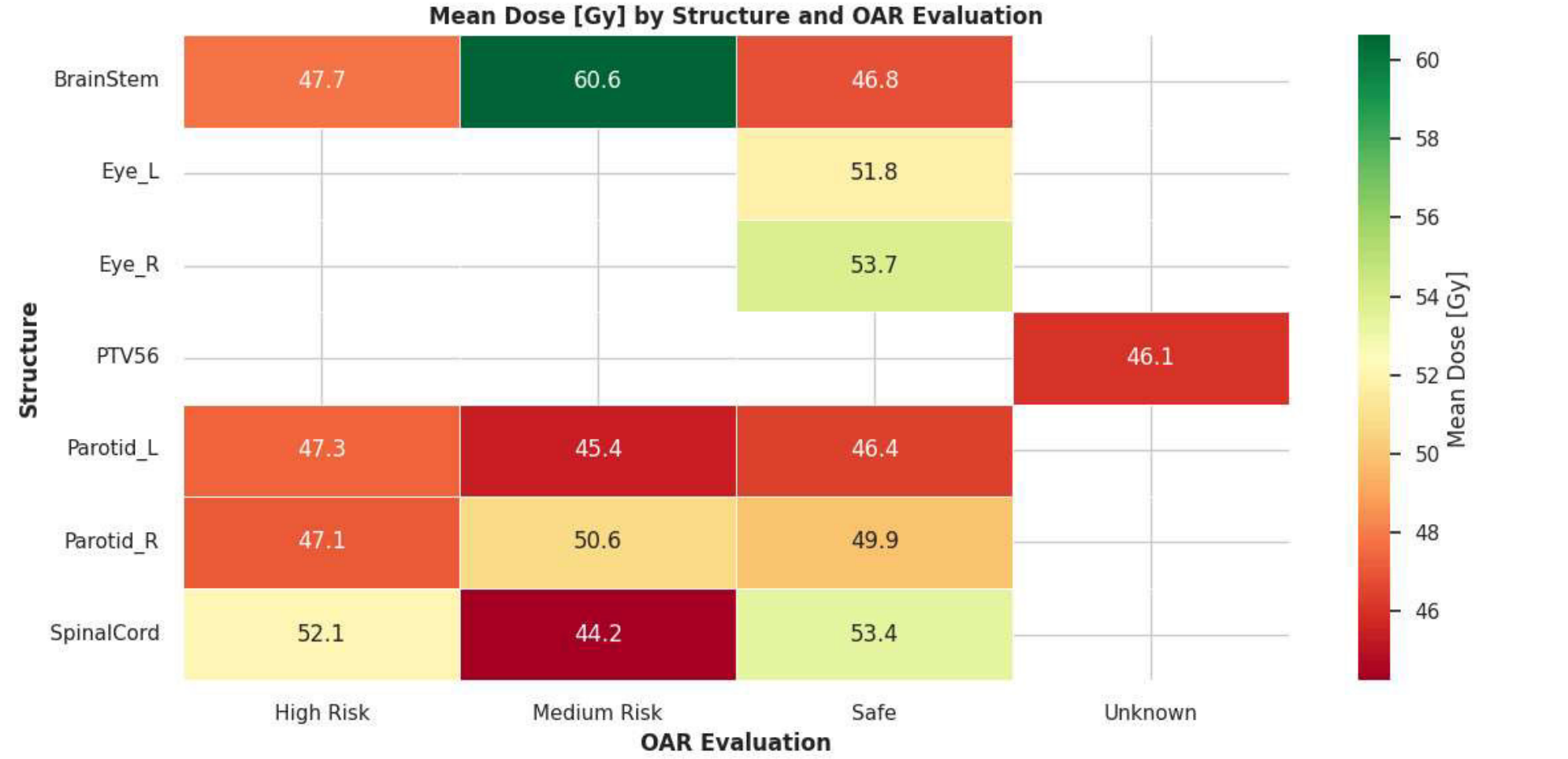


```
dose_cols = ['Min Dose [Gy]', 'Max Dose [Gy]', 'Mean Dose [Gy]',
    'Modal Dose [Gy]', 'Median Dose [Gy]', 'STD [Gy]', 'Conformity Index',
    'Gradient Measure [cm]', 'Dose_@_100%_Relative'
]
plt.figure(figsize=(12, 6))
sns.heatmap(df[dose_cols].corr(), annot=True, cmap='coolwarm', fmt='.2f')
plt.title("Correlation of Dose and Quality Metrics", fontweight='bold')
plt.tight_layout()
```

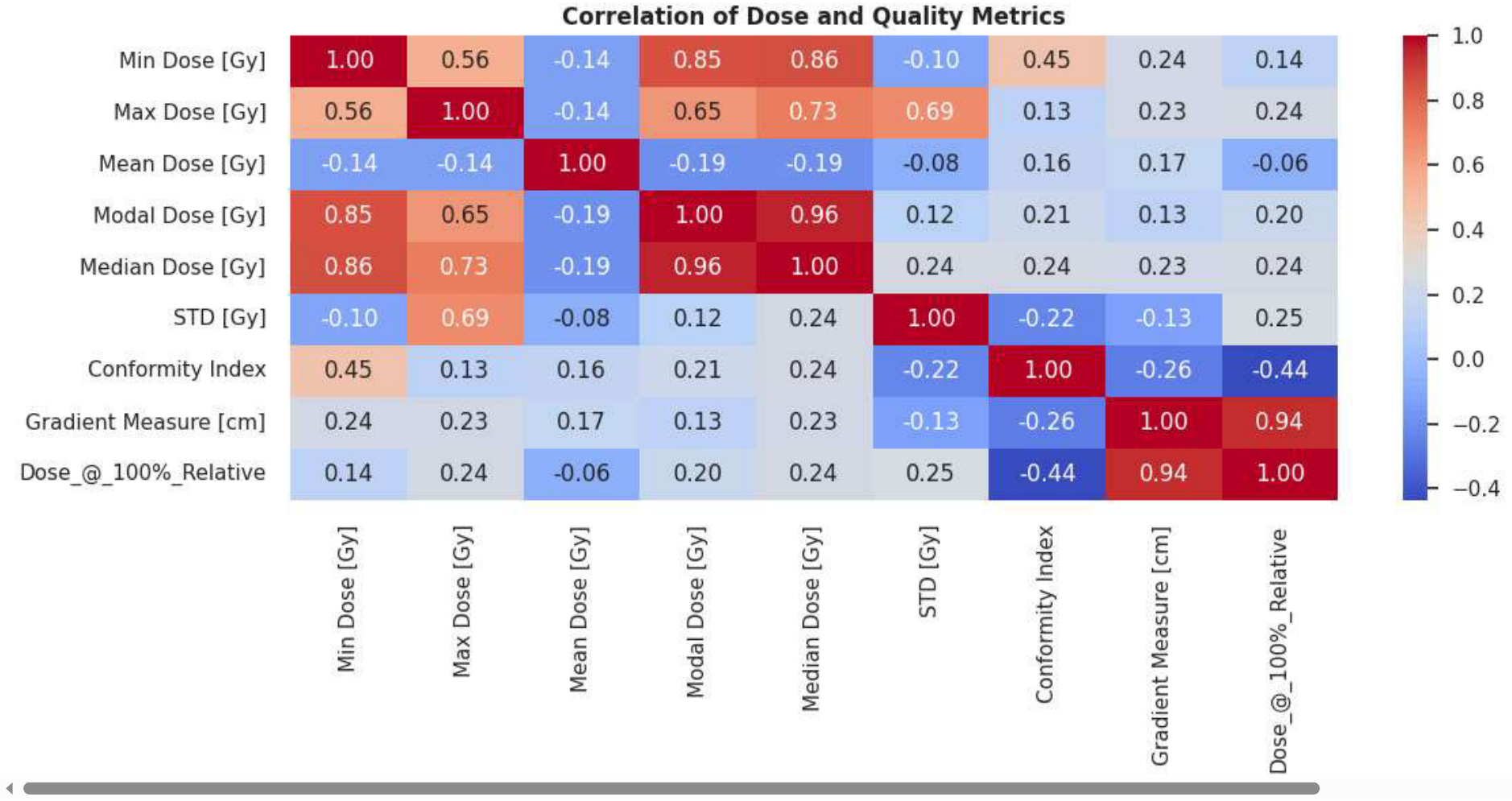


```
sns.pairplot(df, hue='OAR Evaluation', vars=[
    'Mean Dose [Gy]', 'Min Dose [Gy]', 'Max Dose [Gy]',
    'Median Dose [Gy]', 'Conformity Index', 'Gradient Measure [cm]'
])
```

<seaborn.axisgrid.PairGrid at 0x7ef06f65aed0>

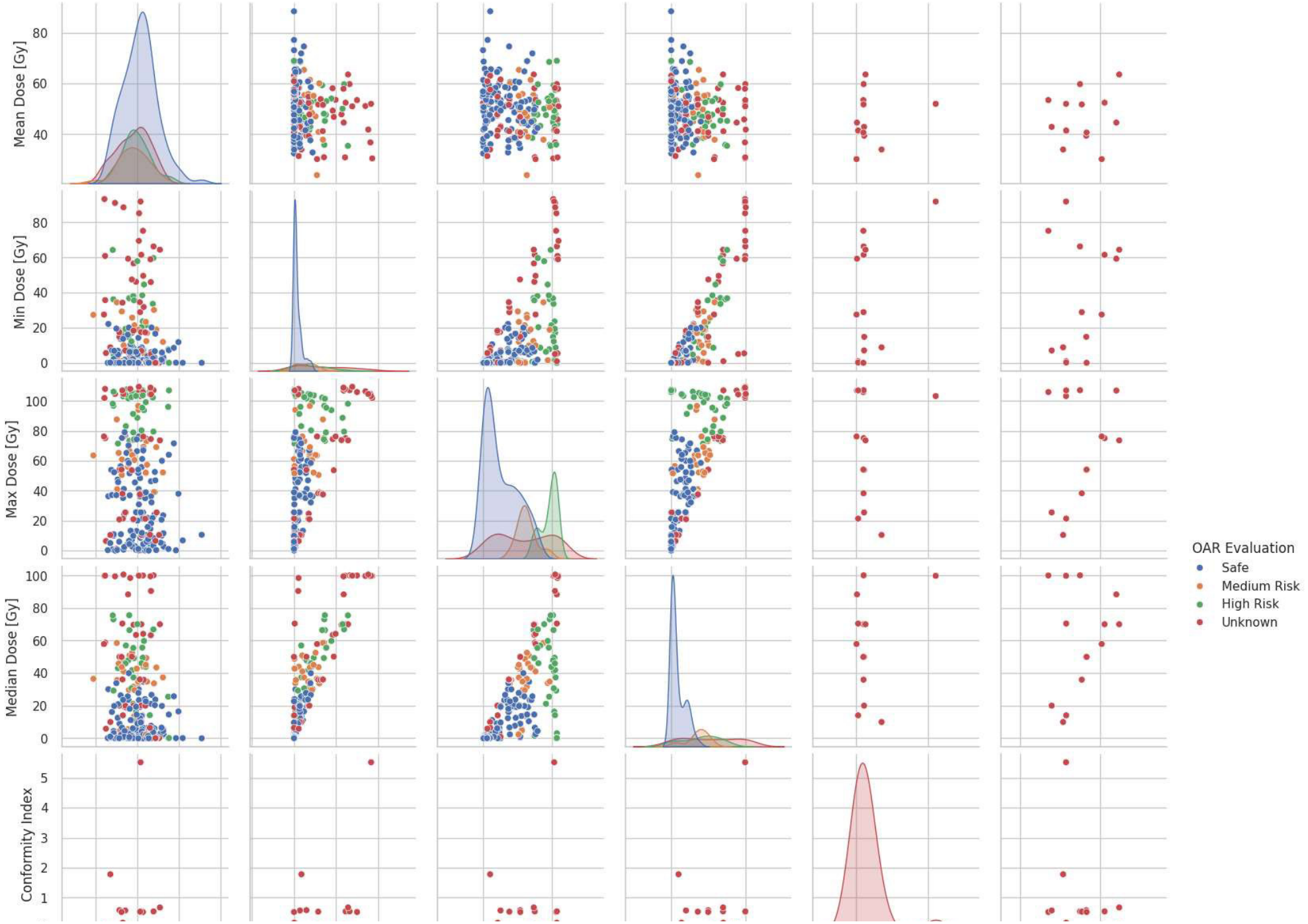

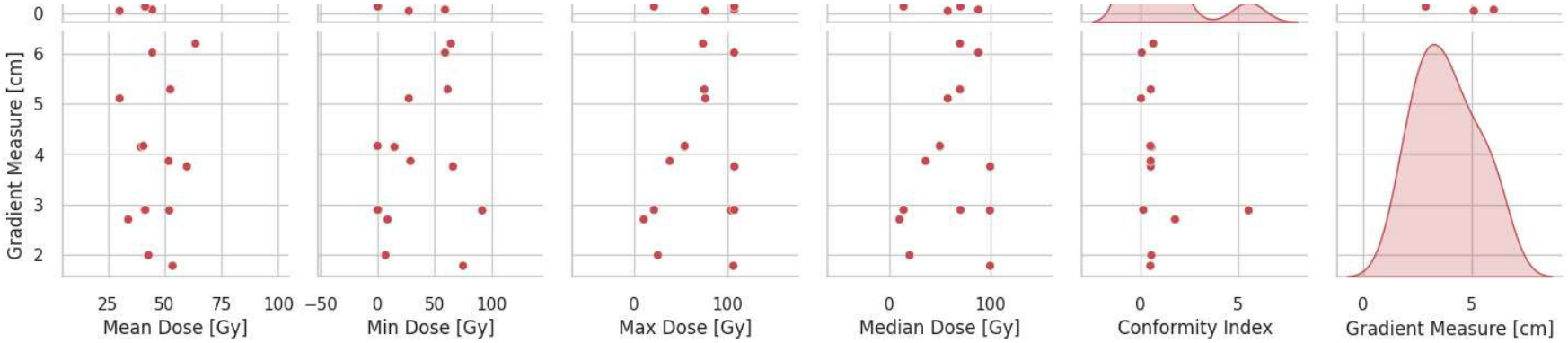


```
plt.figure(figsize=(18, 12))
custom_palette = {
    'High Risk': 'red',
    'Medium Risk': 'orange',
    'Unknown': 'gray',
    'Safe': 'green'
}
for i, col in enumerate(dose_cols, 1):
    plt.subplot(3, 3, i)
    sns.boxplot(data=df, x='OAR Evaluation', y=col, palette=custom_palette)
    plt.title(f'{col} by OAR Evaluation', fontsize=10, fontweight='bold')
    plt.xticks(rotation=30)
    plt.tight_layout()
```

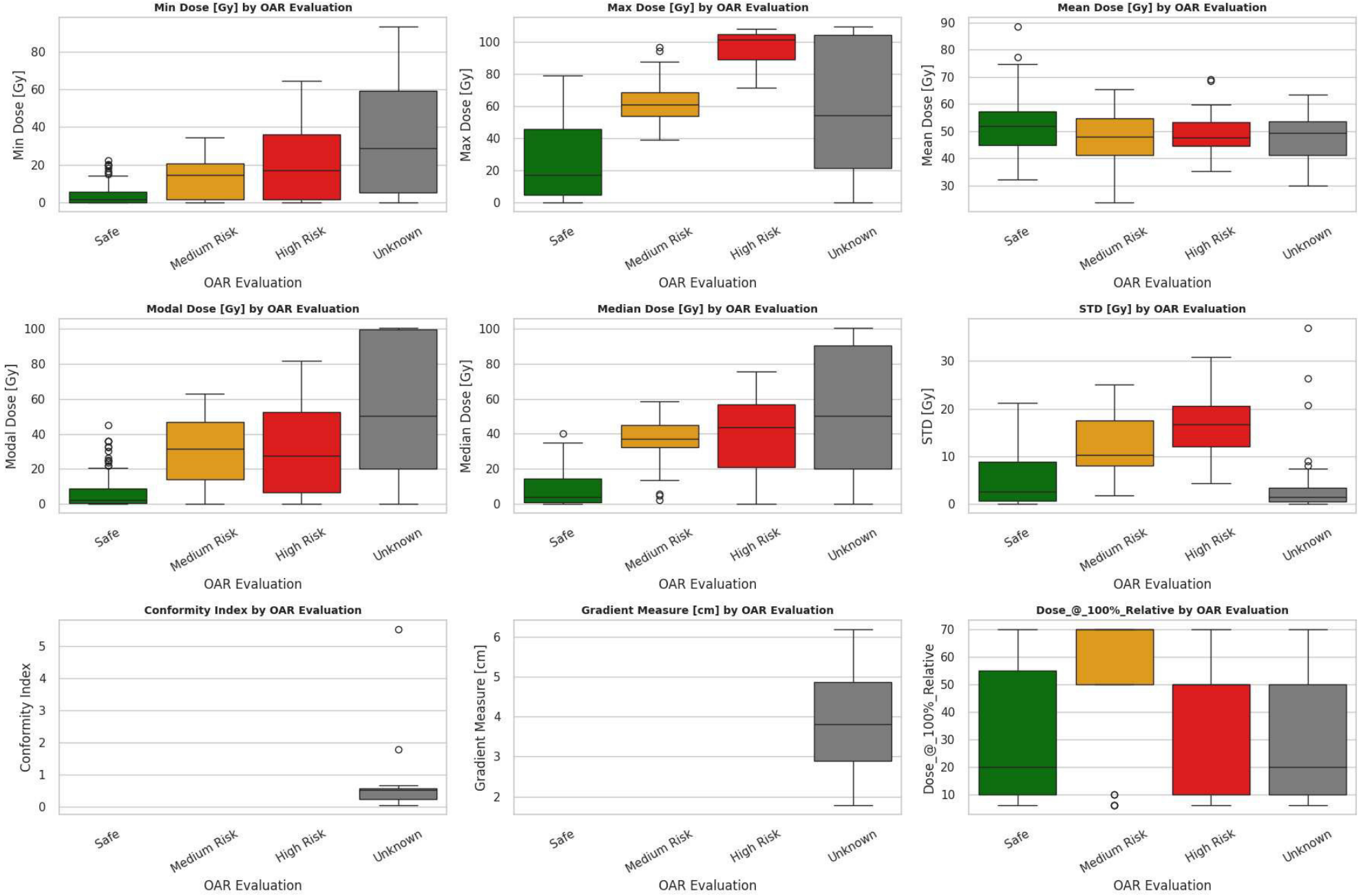
Min Dose [Gy] by OAR Evaluation
Min Dose [Gy]
Max Dose [Gy] by OAR Evaluation
Max Dose [Gy]
Mean Dose [Gy] by OAR Evaluation
Mean Dose [Gy]
Modal Dose [Gy] by OAR Evaluation
Modal Dose [Gy]
Median Dose [Gy] by OAR Evaluation
Median Dose [Gy]
STD [Gy] by OAR Evaluation
STD [Gy]
Conformity Index by OAR Evaluation
Conformity Index
Gradient Measure [cm] by OAR Evaluation
Gradient Measure [cm]
Dose_@_100%_Relative by OAR Evaluation
Dose_@_100%_Relative
Safe
Medium Risk
High Risk
Unknown
OAR Evaluation

```
custom_palette = {
    'High Risk': 'red',
    'Medium Risk': 'orange',
    'Unknown': 'gray',
    'Safe': 'green'
}
sns.barplot(data=df, x='OAR Evaluation', y='Volume [cm³]', estimator='mean', palette=custom_palette)
plt.title("Average Structure Volume by OAR Evaluation", fontweight='bold')
plt.ylabel("Volume [cm³]", fontweight='bold')
plt.tight_layout()
plt.show()
```

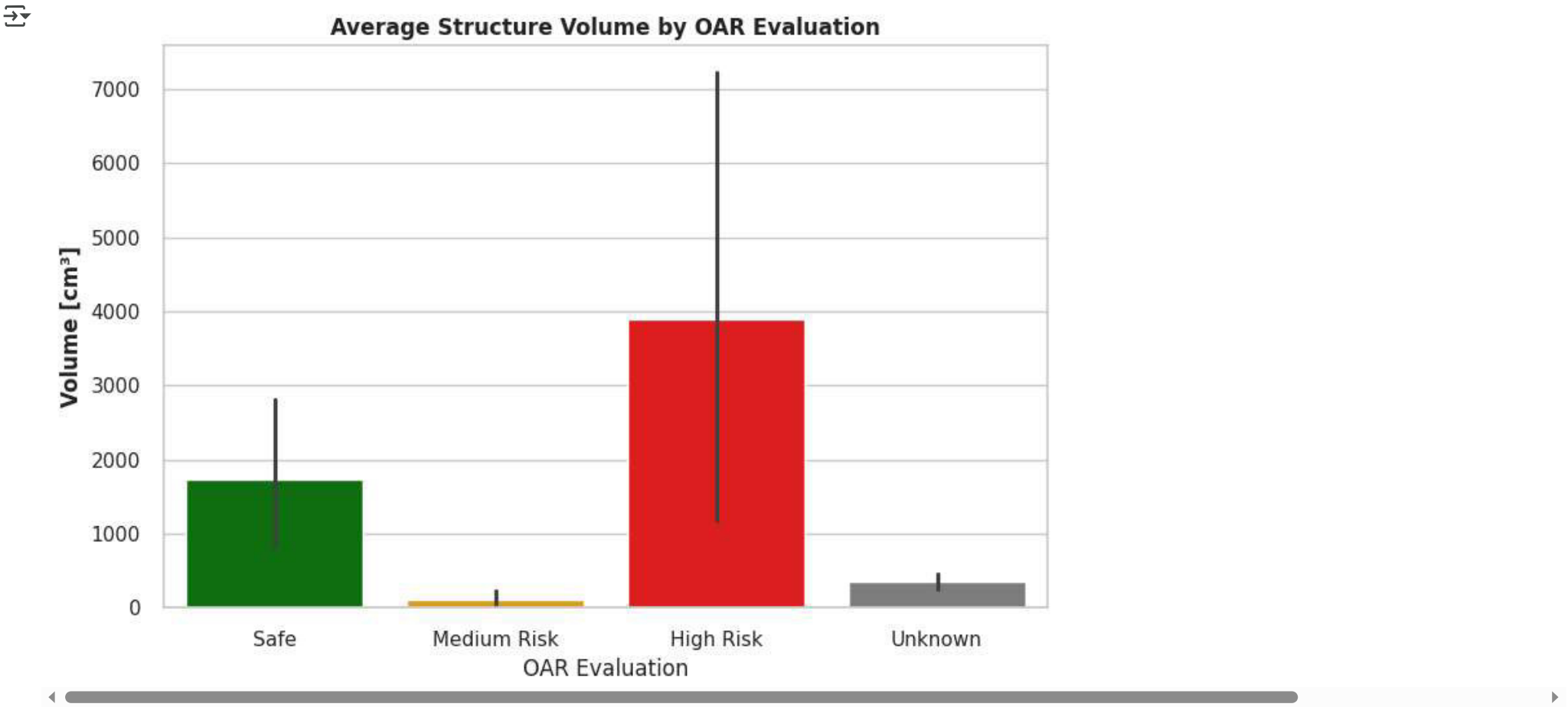

```
from imblearn.over_sampling import RandomOverSampler
from collections import Counter
import pandas as pd

X = data_class.drop(columns=['OAR Evaluation'])
y = data_class['OAR Evaluation']

# 2. Apply Random Oversampling
ros = RandomOverSampler(random_state=123)
X_resampled, y_resampled = ros.fit_resample(X, y)

df_balanced = pd.concat([pd.DataFrame(X_resampled, columns=X.columns),
                         pd.Series(y_resampled, name='OAR Evaluation')], axis=1)

df_balanced['OAR Evaluation'].value_counts(normalize=True)
```

OAR Evaluation	proportion
Safe	0.25
Medium Risk	0.25
High Risk	0.25
Unknown	0.25

dtype: float64

Relative Class Distribution (Before vs After Balancing)

```
# Absolute counts
before_abs = data_class['OAR Evaluation'].value_counts().sort_index()
after_abs = df_balanced['OAR Evaluation'].value_counts().sort_index()

# Relative proportions
before_rel = before_abs / before_abs.sum()
after_rel = after_abs / after_abs.sum()

# Combine into one DataFrame
comparison_df = pd.DataFrame({
    'Before Count': before_abs,
```

```
    'After Count': after_abs,
    'Before %': (before_rel * 100).round(1),
    'After %': (after_rel * 100).round(1)
})

# Reorder rows
comparison_df = comparison_df.sort_index()

comparison_df
```

OAR Evaluation	Before Count	After Count	Before %	After %
High Risk	33	124	14.5	25.0
Medium Risk	26	124	11.4	25.0
Safe	124	124	54.4	25.0
Unknown	45	124	19.7	25.0

Étapes suivantes : Générer du code avec comparison_df | Afficher les graphiques recommandés | New interactive sheet

```
# Relative distribution
before_rel = data_class['OAR Evaluation'].value_counts(normalize=True).sort_index()
after_rel = df_balanced['OAR Evaluation'].value_counts(normalize=True).sort_index()

#Prepare DataFrame
labels = sorted(set(before_rel.index).union(after_rel.index))
df_rel = pd.DataFrame({
    'Class': labels,
    'Before': before_rel.reindex(labels, fill_value=0).values,
    'After': after_rel.reindex(labels, fill_value=0).values
})
df_rel_melt = df_rel.melt(id_vars='Class', var_name='Dataset', value_name='Proportion')

# color palette
custom_palette = ['#1f77b4', '#ff7f0e']

# Plot
plt.figure(figsize=(10, 6))
ax = sns.barplot(
    data=df_rel_melt,
```

```
        x='Class',
        y='Proportion',
        hue='Dataset',
        palette=custom_palette
    )

    #Add percentage labels
    for container in ax.containers:
        ax.bar_label(
            container,
            fmt='%.1f%%',
            labels=[f"{p.get_height()*100:.1f}%" for p in container],
            padding=3,
            fontsize=10,
            fontweight='bold'
        )

    # Styling
    ax.set_title('Relative Class Distribution (Before vs After Balancing)', fontsize=14, fontweight='bold')
    ax.set_xlabel('OAR Evaluation Class', fontsize=12, fontweight='bold')
    ax.set_ylabel('Proportion', fontsize=12, fontweight='bold')
    ax.set_ylim(0, 1)
    ax.tick_params(axis='x', labelsize=11, labelrotation=45)
    ax.tick_params(axis='y', labelsize=11)
    for tick in ax.get_xticklabels() + ax.get_yticklabels():
        tick.set_fontweight('bold')
    plt.grid(axis='y', linestyle='--', alpha=0.7)
    plt.tight_layout()
    plt.show()
```

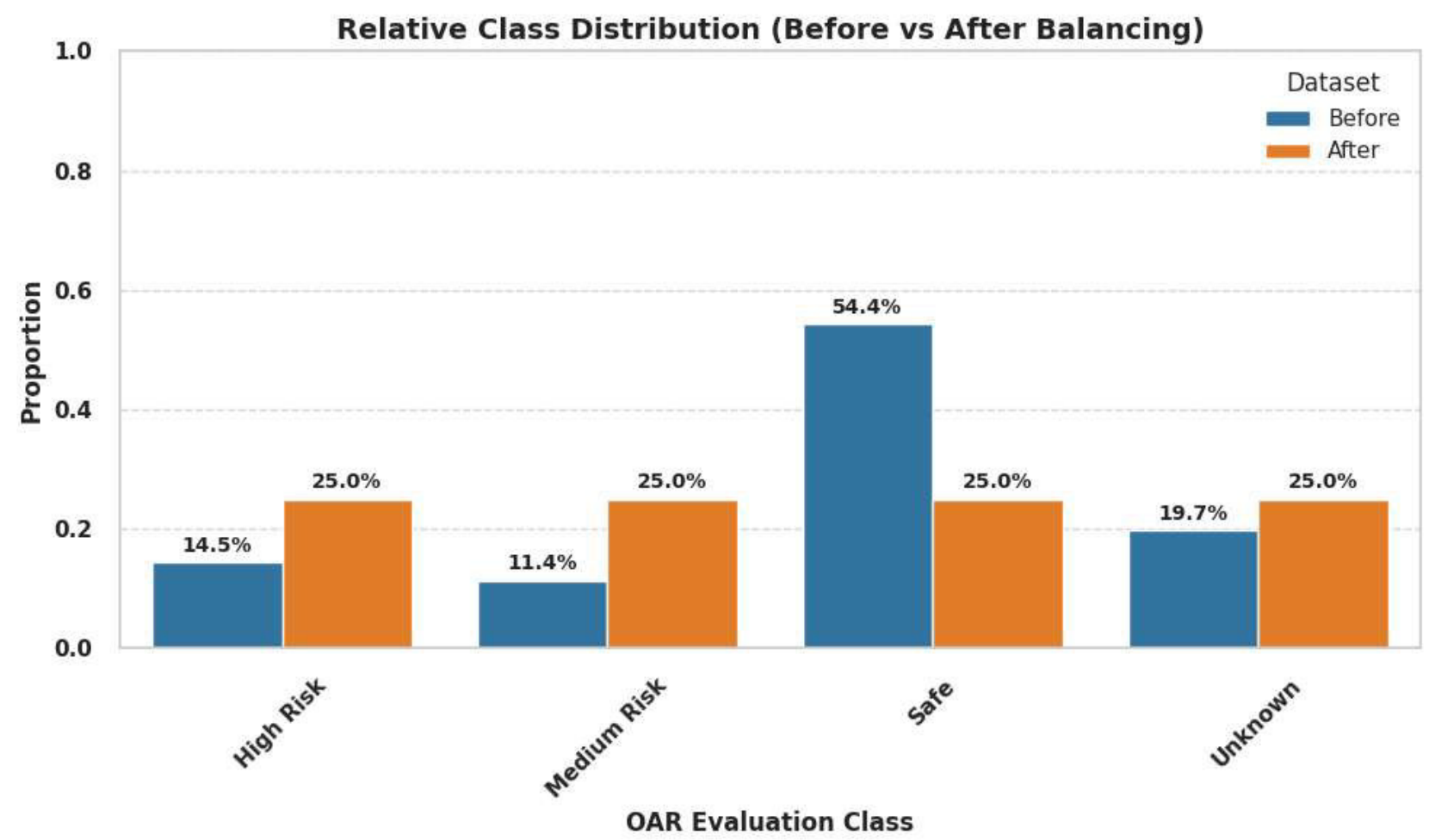

Split Data into Train and Test Sets

```
from sklearn.model_selection import train_test_split

# Y: target / X: features
X = df_balanced.drop(columns=['OAR Evaluation'])
y = df_balanced['OAR Evaluation']

# Data splitting(20%  test,80% train)
X_train, X_test, y_train, y_test = train_test_split(
    X, y, test_size=0.2, random_state=123, stratify=y
```

```
)
```

```
from pycaret.classification import setup, create_model, plot_model
df_train = pd.concat([X_train, y_train], axis=1)

label_map = {
    0: 'Safe',
    1: 'High Risk',
    2: 'Medium Risk',
    3: 'Unknown'
}
if df_train['OAR Evaluation'].dtype in ['int64', 'int32']:
    df_train['OAR Evaluation'] = df_train['OAR Evaluation'].map(label_map)

df_train['OAR Evaluation'] = df_train['OAR Evaluation'].astype('category')
```

Initialize PyCaret on Training Data Only

```
#PyCaret setup
clf_setup = setup(
    data=df_train,
    target='OAR Evaluation',
    session_id=123,
    categorical_features=['Structure Type', 'Approval Status', 'Structure', 'Plan', 'Course'],
    verbose=False
)
```

Compare models

```
best_model_classi =compare_models()
best_model_classi
```

	Model	Accuracy	AUC	Recall	Prec.	F1	Kappa	MCC	TT (Sec)
gbc	Gradient Boosting Classifier	0.9677	0.0000	0.9677	0.9732	0.9671	0.9570	0.9591	0.8100
rf	Random Forest Classifier	0.9640	0.9978	0.9640	0.9688	0.9630	0.9520	0.9541	0.3370
catboost	CatBoost Classifier	0.9640	0.9971	0.9640	0.9688	0.9630	0.9520	0.9541	9.2950
xgboost	Extreme Gradient Boosting	0.9606	0.9957	0.9606	0.9654	0.9596	0.9474	0.9495	0.2420
et	Extra Trees Classifier	0.9566	0.9979	0.9566	0.9651	0.9558	0.9422	0.9455	0.2810
lightgbm	Light Gradient Boosting Machine	0.9536	0.9973	0.9536	0.9587	0.9525	0.9381	0.9402	0.9310
dt	Decision Tree Classifier	0.9317	0.9546	0.9317	0.9448	0.9307	0.9090	0.9139	0.1200
lr	Logistic Regression	0.8951	0.0000	0.8951	0.9114	0.8943	0.8603	0.8659	1.2830
lda	Linear Discriminant Analysis	0.8776	0.0000	0.8776	0.8911	0.8735	0.8369	0.8435	0.1430
ridge	Ridge Classifier	0.8554	0.0000	0.8554	0.8715	0.8472	0.8073	0.8162	0.1490
nb	Naive Bayes	0.8517	0.9587	0.8517	0.8780	0.8439	0.8022	0.8136	0.2490
ada	Ada Boost Classifier	0.8516	0.0000	0.8516	0.8696	0.8490	0.8021	0.8092	0.2150
qda	Quadratic Discriminant Analysis	0.8378	0.0000	0.8378	0.8874	0.8344	0.7838	0.8017	0.2400
knn	K Neighbors Classifier	0.7903	0.9445	0.7903	0.8270	0.7843	0.7207	0.7331	0.1280
svm	SVM - Linear Kernel	0.4476	0.0000	0.4476	0.4861	0.4012	0.2635	0.2948	0.1370
dummy	Dummy Classifier	0.2417	0.5000	0.2417	0.0586	0.0942	0.0000	0.0000	0.1150

```
▸ GradientBoostingClassifier
```

Create and Train the Model

```
best_model = create_model('catboost')
```

```
best_model
```

Fold	Accuracy	AUC	Recall	Prec.	F1	Kappa	MCC
0	0.9643	1.0000	0.9643	0.9688	0.9641	0.9524	0.9540
1	0.8929	0.9932	0.8929	0.9132	0.8839	0.8571	0.8675
2	0.9643	1.0000	0.9643	0.9688	0.9641	0.9524	0.9540
3	0.9643	0.9983	0.9643	0.9688	0.9641	0.9524	0.9540
4	0.9286	0.9796	0.9286	0.9330	0.9284	0.9048	0.9063
5	1.0000	1.0000	1.0000	1.0000	1.0000	1.0000	1.0000
6	1.0000	1.0000	1.0000	1.0000	1.0000	1.0000	1.0000
7	1.0000	1.0000	1.0000	1.0000	1.0000	1.0000	1.0000
8	0.9630	1.0000	0.9630	0.9683	0.9630	0.9506	0.9524
9	0.9630	1.0000	0.9630	0.9676	0.9628	0.9505	0.9523
Mean	0.9640	0.9971	0.9640	0.9688	0.9630	0.9520	0.9541
Std	0.0319	0.0062	0.0319	0.0270	0.0340	0.0426	0.0401

```
<catboost.core.CatBoostClassifier at 0x7ef06e125410>
```

*Finalize the Model *

```
final_model = finalize_model(best_model)
#final_model
```

* Make Predictions on Test Data*

```
test_df = pd.concat([X_test, y_test], axis=1)
predictions = predict_model(final_model, data=test_df)
prediction_col = [col for col in predictions.columns if col.lower() in ['label', 'prediction_label', 'predictions']][0]
y_pred = predictions[prediction_col]
print("Predicted class labels:")
print("Unique predicted labels:", y_pred.unique())
```

	Model	Accuracy	AUC	Recall	Prec.	F1	Kappa	MCC
0	CatBoost Classifier	0.9900	1.0000	0.9900	0.9904	0.9900	0.9867	0.9868

```
Predicted class labels:
377    Medium Risk
291      High Risk
301      High Risk
83            Safe
449        Unknown
Name: prediction_label, dtype: object
Unique predicted labels: ['Medium Risk' 'High Risk' 'Safe' 'Unknown']
```

```
from sklearn.metrics import confusion_matrix, classification_report
if hasattr(y_test, 'cat'):
    labels = list(y_test.cat.categories)
else:
    labels = sorted(y_test.unique())

cm = confusion_matrix(y_test, y_pred, labels=labels)

plt.figure(figsize=(6, 5))
sns.heatmap(cm, annot=True, fmt='d', cmap='viridis',
            xticklabels=labels, yticklabels=labels)

plt.xlabel("Predicted", fontsize=12)
plt.ylabel("Actual", fontsize=12)
plt.yticks(rotation=0)
plt.xticks(rotation=90)
plt.tight_layout()
plt.show()

print("\n🔍 Classification Report:")
print(classification_report(y_test, y_pred, target_names=labels))
```

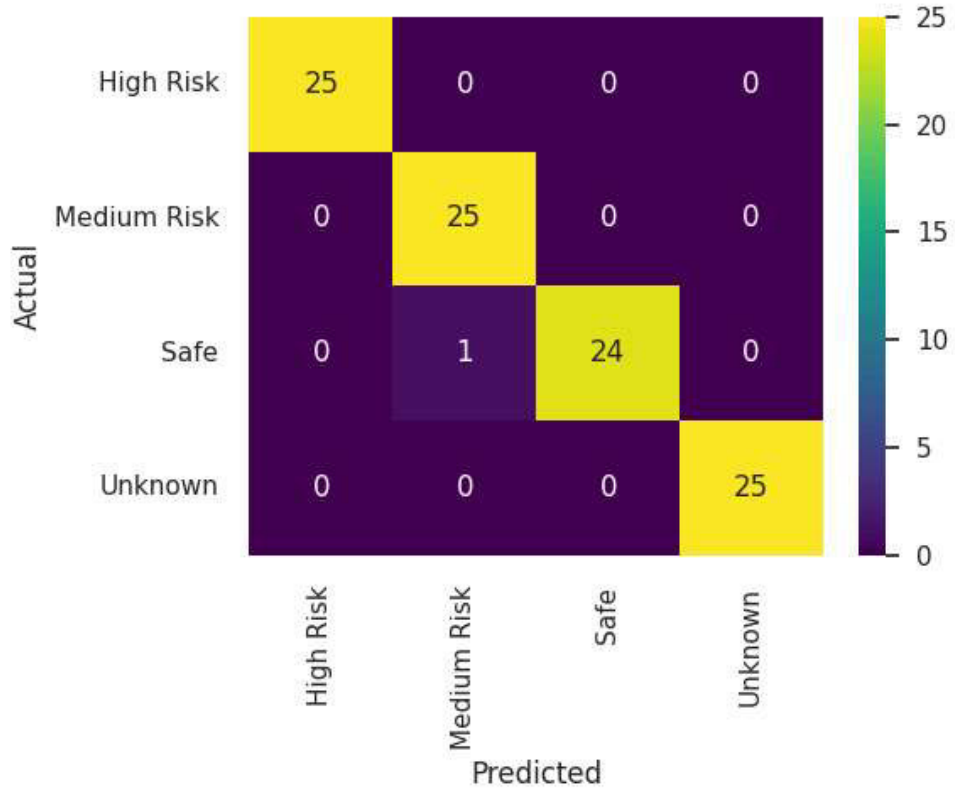

🔍 Classification Report:

	precision	recall	f1-score	support
High Risk	1.00	1.00	1.00	25
Medium Risk	0.96	1.00	0.98	25
Safe	1.00	0.96	0.98	25

Evaluate Model Performance